



Brigham Young University
BYU ScholarsArchive

Theses and Dissertations

2024-04-09

Quantifying and Characterizing the Behavior of Dissolved and Suspended ICP-OES Detectable Elements in Utah Lake

Rachel Ann Valek

Brigham Young University

Follow this and additional works at: <https://scholarsarchive.byu.edu/etd>



Part of the [Engineering Commons](#)

BYU ScholarsArchive Citation

Valek, Rachel Ann, "Quantifying and Characterizing the Behavior of Dissolved and Suspended ICP-OES Detectable Elements in Utah Lake" (2024). *Theses and Dissertations*. 10715.

<https://scholarsarchive.byu.edu/etd/10715>

This Thesis is brought to you for free and open access by BYU ScholarsArchive. It has been accepted for inclusion in Theses and Dissertations by an authorized administrator of BYU ScholarsArchive. For more information, please contact ellen_amatangelo@byu.edu.

Quantifying and Characterizing the Behavior of Dissolved and
Suspended ICP-OES Detectable Elements in Utah Lake

Rachel Ann Valek

A thesis submitted to the faculty of
Brigham Young University
in partial fulfillment of the requirements for the degree of
Master of Science

Gustavious Williams, Chair
Woodruff Miller
Rob Sowby

Department of Civil and Construction Engineering
Brigham Young University

Copyright © 2024 Rachel Ann Valek

All Rights Reserved

Abstract

For Utah Lake in Utah, USA, we analyzed a uniquely comprehensive and longitudinal water quality dataset that extended over two summer sampling seasons. We measured 61 parameters using Inductively Coupled Plasma Optical Emission Spectrometry (ICP-OES), YSI ProDSS water sondes, and laboratory procedures to quantify and characterize dissolved and suspended behavior of trace elements in Utah Lake. We analyzed the data using principal component analysis (PCA) and multidimensional scaling (MDS) to understand the lake geochemistry and inform Utah Lake management decisions regarding nutrients and algal blooms. We found that 1) sediments rich in phosphorus (P) act as a source for bioavailable phosphorus; 2) phytoplankton (as estimated by chlorophyll-a) and cyanobacteria (as estimated by phycocyanin) may not directly respond to bioavailable phosphorus; and 3) potential limiting and colimiting micronutrients such as copper (Cu), nickel (Ni), and zinc (Zn) impact algal growth in Utah Lake. With Cu-based algicides being used as recently as 2021 potential Cu impairment for Utah Lake should be considered in management strategies on the lake. Our MDS analysis indicated that Utah Lake has three distinct geochemical seasons within our sampling periods (May through October): spring (May and June), summer (August), and fall (September). Additionally, our data suggests that Utah Lake aluminum (Al) concentrations using complete digestion are higher than state allowable concentrations, however complete digestion includes Al in suspended clay minerals that are not bioavailable.

Keywords: Utah Lake; Inductively Coupled Plasma Optical Emission Spectrometry; principal component analysis; multiple dimensional scaling; water quality; micronutrient; lake management; trace elements

Acknowledgements

I would like to thank the Utah Division of Forestry, Fire & State Lands and Timpanogos Special Service District for their funding of the data sampling and analysis within this project. Additionally, I would like to thank the Brigham Young University Civil and Construction Engineering Scholarship Society for their financial support throughout my graduate degree, which allowed me to work full time on my research.

I am deeply grateful for the support of my parents, siblings, friends, and loved ones, especially during the most stressful parts of research. I would also like to extend a special thank you to my mentors, Dr. Gustavious P. Williams and Kaylee Tanner, as well as the other members of the Environmental Engineering Laboratory (EEL). Dr. Williams and Kaylee provided vital feedback that helped shape the body of this research. The members of the EEL have become like family to me, accompanying me in gathering and analyzing water samples throughout the summer months. Words cannot adequately express the gratitude I feel for this experience and all the wonderful minds I had the opportunity to work with and be mentored by.

Table of Contents

Abstract.....	ii
Acknowledgements.....	iii
List of Figures.....	vi
List of Tables	viii
1 Introduction.....	1
1.1 Study Overview	1
1.2 ICP-OES DE in aquatic systems.....	2
1.2.1 DE Metals of Concern	2
1.2.2 Other DE Analytes.....	3
1.3 Water Quality Standards Applicable to UL.....	4
2 Materials and Methods.....	7
2.1 Field Study Description.....	7
2.2 Sample Collection.....	8
2.2.1 UL Volume	9
2.2.2 Sediment Samples.....	9
2.3 Probe Measurements.....	11
2.4 Laboratory Analysis Methods	11
2.4.1 Filtration.....	12
2.4.2 Sediment Sample Analysis.....	13
3 Data Summary	14
3.1 Data Nomenclature	14
3.2 Data Cleaning.....	14
3.3 MDL Analysis	16

4 Results	18
4.1 Sediment Data.....	18
4.2 CWA-regulated DE Distributions by Year.....	19
4.2.1 Micronutrients.....	19
4.2.2 Aluminum (Al) and Lead (Pb).....	20
4.2.3 Phosphorus (P).....	21
4.2.4 Barium (Ba).....	22
4.3 Data Analysis	23
4.4 Principal Component Analysis (PCA).....	26
4.4.1 PCA Loading Matrix	27
4.4.2 Variation of PCs over Time	31
4.5 Multidimensional scaling (MDS)	33
5 Discussion.....	37
5.1 Elements.....	37
5.1.1 Copper (Cu) and Nickel (Ni)	37
5.1.2 Zinc (Zn)	38
5.1.3 Aluminum (Al)	39
5.1.4 Phosphorus (P).....	39
5.1.5 Barium (Ba).....	40
5.2 Chlorophyll-a (Chl-a) and Phycocyanin (PhC)	40
6 Conclusions	42
References	44
Appendix	54

List of Figures

Figure 2-1. Study locations: 0.4 km (0.25 mi) offshore, northwest of Lindon marina.	8
Figure 2-2. Water sampling.....	9
Figure 2-3. Sediment and water sample locations.	10
Figure 3-1. Field sampling frequency for 2021 and 2022 sampling seasons.	16
Figure 3-2. Percentage of samples for each ICP-OES analyte with measured concentrations above the MDL. Analytes with 100% detection in both filtered and unfiltered samples excluded.	17
Figure 4-1. Distributions of (A) Cu, (B) Zn, and (C) Ni grouped by year, 2021 and 2022; and phase, unfiltered (dark blue) and filtered (light blue). The plots include reference lines for acute (light green) and chronic (dark green) regulatory values. *Note: when acute and chronic standards are the same only the chronic regulatory values are visible (e.g. Zn).	20
Figure 4-2. Distributions of (A) Al and (B) Pb grouped by year, 2021 and 2022; and phase, unfiltered (dark blue) and filtered (light blue) with reference lines for acute and chronic regulatory levels.....	21
Figure 4-3. Distributions of P grouped by year, 2021 and 2022; and phase, unfiltered (dark blue) and filtered (light blue) with reference lines for acute and chronic regulatory levels.	22
Figure 4-4. Distributions of Ba grouped by year, 2021 and 2022; and phase, unfiltered (dark blue) and filtered (light blue) with reference lines for acute and chronic regulatory levels.	22
Figure 4-5. Correlation heatmap showing the pair-wise correlation among all 61 parameters. All pairs with correlations greater than 0.7 are outlined in dark gray excluding the correlations of 1 on the diagonal of the square	

matrix which is the correlation of the parameter with itself and is always	
1.....	24
Figure 4-6. (A) The first 27 PCA eigenvalues. (B) PCA Scree Plot of the	
original 61 parameter dataset.	27
Figure 4-7. PC loading matrix. Weights above 0.5 are outlined in dark	
gray.....	29
Figure 4-8. As_U cyclical trend.....	31
Figure 4-9. PC 1, 2, and 5 values through time for the 2021 (A) and 2022	
(B) sampling seasons.....	32
Figure 4-10. PC 3 and 4 timelines for the 2021 (A) and 2022 (B) sampling	
seasons.	33
Figure 4-11. (A) Euclidean MDS scaling plot for the 61-parameter data	
using z-score standardization. (B) Euclidean MDS scaling plot for the 27	
PCs. Each plot shows all 28 samples.....	34
Figure 4-12. MDS data groupings for the z-score dataset.....	36
Figure A-1. Distributions of (A) As, (B) B, (C) Cd, (D) Cr, (E) Fe, and (F) Se	
grouped by year, 2021 and 2022; and phase, unfiltered (dark blue) and	
filtered (light blue) with reference lines for acute and chronic regulatory	
levels.....	54

List of Tables

Table 1-1. Most stringent applicable standard for each regulated element in UL.....	6
Table 2-1. YSI ProDSS sonde parameter accuracy and resolution [91-95].	11
Table 2-2. Lab analytes and methods.....	11
Table 2-3. ICP-OES minimum detection limits (MDLs).....	12
Table 2-4. Filter contaminants.....	12
Table 3-1. Parameter abbreviations.....	14
Table 3-2. Data replacement methods.	15
Table 4-1. Average concentrations of DEs in UL sediments listed in descending concentration order.	18
Table 4-2. Pair-wise Pearson correlation coefficients (PCC) for all pairs with values greater than 0.7.....	25
Table 4-3. PC reference table. Parameters with significant weights (>0.5) within each PC are listed for both positive and negative correlations.	28
Table 4-4. Shepherd diagram fit details for the z-score standardized and PC datasets.	35

1 Introduction

1.1 Study Overview

Utah Lake (UL) is a shallow, turbid, eutrophic, and slightly saline lake in north-central Utah. It is Utah's largest freshwater lake by area and a valuable natural resource with a unique, highly productive ecosystem that faces challenges related to historic pollution, invasive species, harmful algal blooms (HABs), and controversy over management strategies.

The lake is approximately 40 km by 21 km, with a surface area of 390 km² at maximum fill. It is extremely shallow, with an average depth of only 3 m when full. The lake's shallowness, combined with its long fetch and situation in the path of valley winds, results in persistently choppy water which prevents stratification of the water column and, which, coupled with bioturbation from carp, continually resuspends lakebed sediment. Nearly 50% of inflow is lost to evaporation, increasing water column TDS and alkalinity. UL waters are near the solubility limit of calcite, with an estimated 50% of the inflow of dissolved calcium and bicarbonate precipitating in the lake [1]. The lake's highly turbid water, full of suspended sediments, dissolved minerals, and nutrients, drives many of its geochemical, ecological, and hydrologic functions.

Although there is a relatively extensive, long-term body of research and data on UL, much of the focus has been on ecology—particularly the highly variable but intense and sometimes toxic algal blooms that occur in the lake. The earliest publication on UL algae is from 1931 [2], with many publications on algal taxa and communities published in the 1960's through the present [3-12]. Additionally, there has been significant work on nutrient loads [13-20] and geologic materials [21-23]. Some of the earliest published work using earth observation satellites to study water quality was on UL, beginning in the early 1970s. UL was a case study presented in some of the first papers using data from NASA's Landsat satellite in the early 1970s [24, 25], with another early remote sensing paper in the 1980s using UL to demonstrate the Heat Capacity Mapping Mission (HCMM) [26] and AVHRR sensor [27]. More recent remote sensing work has focused on long-term trends, variability, and seasonal methods [28-38].

Despite this large body of work, metals in the water column, which have significant impacts on general water quality and ecological function, are not well-researched in UL. A study from 2014 investigated arsenic and other heavy metals in Utah Lake and its tributaries but was

primarily focused on compliance with EPA standards and identifying sources of pollution [39]. Although heavy metal pollution is a significant concern, metals have many functions in aquatic systems, including providing micronutrients for aquatic life [40-42] and affecting geochemical reactions [43]. Because of these varied but substantial impacts on water quality and ecosystem health (which are further detailed in Section 1.2), the lack of information on metals in the UL water column is a critical gap in scientific knowledge of the lake.

Studies worldwide have investigated concentrations and impacts of trace metals in aquatic systems [44, 45]. Bayer, et al. [46] completed a water quality assessment for Lake Hayes in New Zealand focused on the biological importance of macro- and micronutrients. This study conducted bioassays with nitrogen (N), phosphorus (P), copper (Cu), iron (Fe), boron (B), molybdenum (Mo), zinc (Zn), and silicon (Si) trace elements. They found that N, Zn, and B—rather than P—limit phytoplankton growth in Lake Hayes. Dengg, et al. [47] similarly studied the potential colimitation of trace elements manganese (Mn), cobalt (Co), Fe, Zn, and Mo in Taupo Volcanic Zone (TVZ) in New Zealand and found that Fe was a colimiting micronutrient for cyanobacteria in two lakes within the TVZ area. Similar studies in southeastern Australia indicate that trace micronutrients are “an important regulator of the severity of cyanobacterial blooms” [48, 49]. Studies of trace micronutrients within an aquatic ecosystem are essential for effective management of HABs in water bodies as they identify the nutrients and other factors that may be controlling phytoplankton and cyanobacterial growth.

We provide the first characterization of Inductively Coupled Plasma Optical Emission Spectrometry (ICP-OES) detectable elements (DE), including several heavy metal and nonmetal elements in UL on both dissolved and suspended concentrations of DE in the UL water column collected over two summer sampling periods. We analyzed the influence of water column conditions on DE concentrations with principal component analysis (PCA) and multidimensional scaling (MDS) to better understand the geochemical environment of the UL water column. These data and analyses provide a greater understanding of ambient concentrations of total and dissolved DE in the UL water column by showing how they are correlated with each other and with other water quality parameters as well as how the DE are distributed between the total and dissolved phases. This knowledge will inform proposed management strategies and restoration efforts which are currently under consideration for the lake.

1.2 ICP-OES DE in aquatic systems

1.2.1 DE Metals of Concern

Metals are a natural part of the environment and are present in all ecosystems. Natural concentrations for metals in water bodies change based on the geology, land use, erosion, and geochemistry. Aquatic biota ingest or absorb metals and both affect and are affected by concentrations. There are typically no visible indicators of the presence of metals in surface waters like there are for nutrients and sediment, although at toxic or deficient levels there can be visually apparent impacts such as physiological damage to wildlife [50].

All metals become toxic to aquatic life at certain thresholds [51]. When metals reach toxic concentrations in biological systems, they impair the survival, reproduction, and behavior of aquatic life. Some metals and metalloids that commonly cause toxic effects at concentrations

found in the environment include arsenic (As), cadmium (Cd), chromium (Cr), lead (Pb), nickel (Ni), selenium (Se), Cu, and Zn [50]. Even in lower concentrations, metals such as As, Cd, and Pb, can affect mobility, feeding, and navigation behaviors of both terrestrial and aquatic invertebrates [52-54]. As invertebrates are the core of many food chains, these effects ripple throughout the entire aquatic ecosystem [55, 56]. In larger organisms such as fish, Pb, Cd, Ni, and Cr can impact growth rates, biological processes, and reproductive health [57, 58]. Impacts of aluminum (Al), Cd, Cu, Zn, Pb, Ni, As, and Se on birds include behavioral impairments and reduced reproductive success [59-61]. Metals toxicity is a particular concern for UL as it hosts a large migratory bird population along with the endemic and threatened June Sucker fish species.

Some metals exhibit both toxic excess levels and toxic deficient concentrations. Zn, Cu, and Ni, negatively impact biological activity if they are present in excess levels as well as at toxic deficit concentration levels [40-42, 55, 56, 62]. Some metals, such as B, Fe, Mn, and Mo, act as micronutrients and are essential for aquatic life, and in several studies, micronutrients have been found to be limiting or colimiting variables to algal growth [46, 63-66]. In 2008, Downs, et al. [42] conducted a review of micronutrients in 56 freshwater lakes and found that “the proportion of the lakes analyzed in which micronutrient limitation was found was 76% for molybdenum; 74% for iron; 67% for boron, 67% for cobalt, and 20% for copper.” Similar to the effects of toxicity, nutrient deficiencies for algae and phytoplankton growth affect the entire biota of lake systems, including invertebrates, migratory birds, fish, and other organisms [55, 56].

The US Environmental Protection Agency (EPA) lists the following sources and activities as candidate causes for impairment related to heavy metals and other potentially harmful elements: mines and smelters, firing ranges, municipal waste treatment outfalls, industrial point sources, urban runoff, landfills, and junkyards [50]. Other sources include combustion of fossil fuels, phosphate fertilizers, metallo-pesticides, and road salts [51, 67].

All of these sources have been, or are currently are present within the UL watershed. There are seven wastewater treatment plants (WWTP) that discharge effluent directly or indirectly into the lake [68]. The southern end of UL is surrounded by agricultural land, and the western side has several currently active gravel mines. The population in the area immediately surrounding UL, Utah County, has nearly tripled over the last four decades, increasing from ~220,000 in 1980 to ~640,000 in 2020 [69]. This dramatic increase in development and human activity has likely increased the loading of metals to UL related to urban runoff.

In addition to these current sources, the Geneva Steel plant, the largest integrated steel plant in the western United States, operated from 1944 to 2002 on the northeastern shore of UL. This plant produced steel using “coal-derived coke,” with effluent drains near the lake that served as a substantial source of metals to UL [70-72].

The presence of such a variety and quantity of sources around UL underscores the importance of characterizing metals in the UL ecosystem and assessing their impacts on the health of the lake.

1.2.2 Other DE Analytes

In addition, ICP-OES measures several other elements that have important functions or impacts on aquatic ecosystems, including barium (Ba), calcium (Ca), potassium (K), sodium (Na), sulfur (S), B, Si and P.

B and S occur naturally in aquatic environments and are essential nutrients, although anthropogenic activities can elevate their concentrations to toxic levels [73-75]. While S concentrations must be quite high to cause toxic effects, the range between toxic deficit and excess concentrations of B is small when compared to other nutrients [76].

Ba occurs naturally and is also released by industrial processes—primarily as airborne particles that enter surface waters through atmospheric deposition, which UL is particularly susceptible to due to its location and large surface area. Ba is highly reactive and usually exists in aqueous systems as a precipitated form, either as an insoluble sulfate or as carbonate salts. Alkaline environments such as UL further limit its solubility [77].

K and P are key nutrients for aquatic primary production, although plants need much less K than they do P so K is not usually a limiting nutrient. Neither element becomes toxic at the concentrations found in surface waters, although high concentrations of P can fuel eutrophication, which degrades water quality. Natural sources include weathering of phosphate-bearing rocks and geologic mineralized formations. The Delle Phosphatic and Meade Peak geologic formations within the UL watershed contribute large amounts of P to the lake through natural weathering of the P-bearing rocks and soil [20, 78, 79]. The origin and behavior of P in UL is currently a subject of much debate and ongoing research.

Ca and Si are essential micronutrients that are abundant in UL due to the surrounding geology. Ca is a key component of water hardness, and its tendency to form compounds with many other elements makes it an important when characterizing water column geochemistry. Si is generally harmless even at very high concentrations, but it can sometimes inhibit algal growth if present in extremely high concentrations.

Na is a key component of salinity and can severely degrade freshwater systems if present in high concentrations. It enters surface waters through the natural weathering, but also from road salts [80].

The impacts of Se are not well understood in freshwater systems, due to the complexity of its geochemical interactions and cycling, but it is toxic at very low concentrations and has been found to degrade aquatic systems when it enters surface waters through anthropogenic activity [81]. While Se is necessary for aquatic biota there is a very narrow concentration window in which Se turns from necessary to toxic [82].

These discussions on the origins and impacts DE on the UL ecosystem are not comprehensive and vary with each plant and animal species, specific DE, and concentration, among other factors. We included this review to demonstrate the potential impacts and functions of these DE in the UL ecosystem and illustrates the importance of understanding their ambient concentrations and behaviors.

1.3 Water Quality Standards Applicable to UL

We analyzed 25 elements, 12 of which are regulated by water quality standards promulgated by the Division of Water Quality of the Utah Department of Environmental Quality in compliance with the Clean Water Act [83-85]. To contextualize our discussion of water column concentrations, we outline the relevant standards.

The Standards of Quality for Waters of the State [83-85] categorizes waterbodies according to their use and significance and prescribes different standards for each category. UL is classified as:

- 2A: "Protected for frequent primary contact recreation where there is a high likelihood of ingestion of water or a high degree of bodily contact with the water" (swimming, kayaking, diving, water skiing, etc.);
- 2B: "Protected for infrequent primary contact recreation. Also protected for secondary contact recreation where there is a low likelihood of ingestion of water or a low degree of bodily contact with water" (e.g. boating, wading, etc.) [85];
- 3B: "Protected for warm-water species of game fish and other warm water aquatic life, including the necessary aquatic organisms in their food chain;"
- 3D: "Protected for waterfowl, shore birds, and other water-oriented wildlife not included in Classes 3A, 3B, or 3C, including the necessary aquatic organisms in their food chain;"
- 4: "Protected for agricultural uses including irrigation of crops and stock watering"[83-85].

For the 3B and 3D standards, the regulations for dissolved elements are in units of $\mu\text{g}/\text{L}$. For class 4 standards, dissolved elements are in units of mg/L . We converted the 3B and 3D standards to units of mg/L to match our data units.

Al, Cd, Cr, Cu, Ni, Pb, and Zn standards depend on water hardness, called "hardness dependencies". Using data from the Utah Ambient Water Quality Management System (AWQMS) collected from 1978 to 2015, the mean hardness of UL water is 197.4 mg/L as CaCO_3 with a range from 123 to 291 mg/L . We used the mean value to calculate a reference concentration for elements with hardness dependencies for discussions. For Cd, Cr, Pb, and Zn, the conversion is a natural log equation based on the hardness of the water with a specified conversion factor [83].

For Al, since the pH of the lake water is nearly always greater than 7.0 and the hardness is greater than 50 mg/L as CaCO_3 , we use the acute Al criterion of 750 $\mu\text{g}/\text{L}$ (expressed as total recoverable Al) for our discussion. The Utah Department of Water Quality (UDWQ) is currently in the process of adopting the EPA's recommended Al criteria, which depends on dissolved organic carbon (DOC), hardness, and pH. We were told in conversations with representatives of UDWQ that the current value of 750 $\mu\text{g}/\text{L}$ is acceptable as a reference point [86]. Al and P are the only regulated elements with a standard for total recoverable concentration—all other elements require analysis of dissolved concentrations.

Setting criteria for Al is complex, as clay minerals, which make up a significant fraction of suspended solids, have high Al concentrations, but this Al is not bioavailable or reactive. We analyzed filtered and unfiltered samples. We performed a complete digestion of the unfiltered samples which includes the clay minerals. The filtered samples only measure dissolved elements. We did not attempt to follow UDWQ analysis methods but were not able to determine if the UDWQ's definition of "total recoverable Al" required unfiltered lake water to be analyzed after aggressive acid digestion, which would include the nonreactive Al bound up in clay particles in the results, or if they intended for only filtered sample to be analyzed, which would measure only

dissolved, presumably bioavailable Al. We performed both types of analysis on all our samples and present results for total concentrations, which include the Al associated with clay, and dissolved concentrations in this study.

Table 1-1 lists the acute (1-hr average) and chronic (4-day average) standards for the 12 regulated DE analytes [83].

Table 1-1. Most stringent applicable standard for each regulated element in UL.

DE	Acute Standard (mg/L)	Chronic Standard (mg/L)	Designated Use
*Aluminum (Al)	0.75	0.75	3B, 3D
**Arsenic (As)	0.10	0.10	4
**Boron (B)	0.75	0.75	4
Cadmium (Cd)	0.0018	0.00072	3B, 3D
***Chromium (Cr) (Hexavalent)	0.016	0.011	3B, 3D
Copper (Cu)	0.013	0.009	3B, 3D
**Iron (Fe)	1	1	3B, 3D
Nickel (Ni)	0.468	0.052	3B, 3D
*Phosphorus (P)	0.025	0.025	3B
Lead (Pb)	0.065	0.0025	3B, 3D
Selenium (Se)	0.0184	0.0046	3B, 3D
Zinc (Zn)	0.12	0.12	3B, 3D

* DE whose standards are based on total recovery criteria

**Measured as maximum not acute and chronic

***We measured elemental Cr, not hexavalent

2 Materials and Methods

2.1 Field Study Description

We collected water samples approximately once per week on UL over two sampling seasons: June–October 2021 and May–August 2022. This sampling campaign was associated with mesocosm water quality studies [87, 88]. We collected our lake background samples near but outside the mesocosms, roughly 400 m offshore at the northeast end of the lake at approximately 40.33304° Latitude and -111.77509° Longitude for both sampling seasons (Figure 2-1). These samples represent typical water column conditions in the northeastern part of UL.

At the beginning of the 2021 and 2022 sampling seasons, the depth of the water column was 2.5 m at the sample location, which is a typical depth for the lake at that distance from shore. By the end of the season, the depth was 1.5 m as the lake levels decreased due to evaporation and outflow through the Jordan River. The seasonal pattern of drawdown and refill is also typical for the lake.

We analyzed the samples using ICP-OES analysis on a Thermo-Scientific iCAP7400 for both dissolved (filtered on a 0.45-micron filter) and total (unfiltered) samples. We measured total suspended solids (TSS), volatile suspended solids (VSS), and total dissolved solids (TDS) for each sample at the Timpanogos Special Services District’s Environmental Laboratory. Coincident with the water samples, we used YSI ProDSS water quality sondes to collect data on optical dissolved oxygen (ODO), turbidity (TU), specific conductance (SpC), water temperature (WT), pH, chlorophyll-a (Chl-a), and phycocyanin (PhC). This long, high-frequency dataset on water quality and conditions in UL allows us to analyze variation, trends, correlations, and prevailing conditions to characterize DE concentrations in UL.

This is a unique and comprehensive longitudinal dataset for UL, with near-weekly samples collected on 28 days over two summer sampling campaigns. We analyzed the samples for 61 different parameters on highly sensitive laboratory equipment. While spatially limited to the northeastern corner of the lake, we assume these data characterize general conditions in UL. The purpose of our study is to begin to characterize and understand the presence and behaviors of ICP-OES detectable elements in UL.



Figure 2-1. Study locations: 0.4 km (0.25 mi) offshore, northwest of Lindon marina.

2.2 Sample Collection

Over the two sampling seasons, weather permitting, we collected water samples on a weekly basis. The sample season lasted from June to October in 2021 ($n = 15$) and from May to August in 2022 ($n = 13$). We followed procedures from the “Standard Operating Procedure for Lake Water Sampling and Data Collection” from the UDEQ [37].

We used 1 L dip samplers (Figure 2-2) that were triple rinsed in lake water at the sample location prior to collecting the sample. After the triple rinse, we inverted the dip sampler and submerged it until the bottom of the sampler cup was just below the water surface. We then inverted the sample cup to fill it with water. This method reduced the amount of potential contamination from surface scum or floating particles. We used the collected water to triple rinse a new, pre-labeled, opaque 250 mL plastic sample bottle, then filled the bottle to the top, leaving no headspace, and immediately placed it on ice in a cooler. Samples were either analyzed or frozen within a few hours of collection.

For probe measurements, we fully submerged YSI ProDSS water quality sondes at the lake sample location and logged the sensor data at a depth of ~30 cm. We calibrated probe sensors at the end of every week following YSI standards [89]. We analyzed the sensor drift by comparing readings before and after calibration. We found weekly drift in the probe sensors was minimal—smaller than the uncertainty range of the sensors. Based on this result we determined to use weekly rather than daily calibration. Weekly calibration provided a significant cost and time savings and did not affect the reliability of the measurements as evidenced by the negligible sensor drift.

2.2.1 UL Volume

We obtained UL volume data from the Bureau of Reclamation (BOR) which provides daily volumes based on the lake's surface elevation since January of 1932 [90]. We used data that corresponded with the water samples collection dates. We included volumes data as UL volumes vary greatly and we expect volume to impact DE concentrations.



Figure 2-2. Water sampling.

2.2.2 Sediment Samples

During the 2022 sampling season, we collected twelve sediment samples near the water sampling location and across the lake (Figure 2-3). We collected these sediment samples from the first couple of centimeters of the lakebed with a shovel in shallow locations or with an Eckman dredge in deeper locations. On August 3rd, 2022, we took a total of three sediment samples near the water sample. On September 6th, 2022, we took six sediment samples across the center line of UL (Figure 2-3). We collected the last three sediment samples on November 1st, 2022, just north of the Utah Lake State Park.

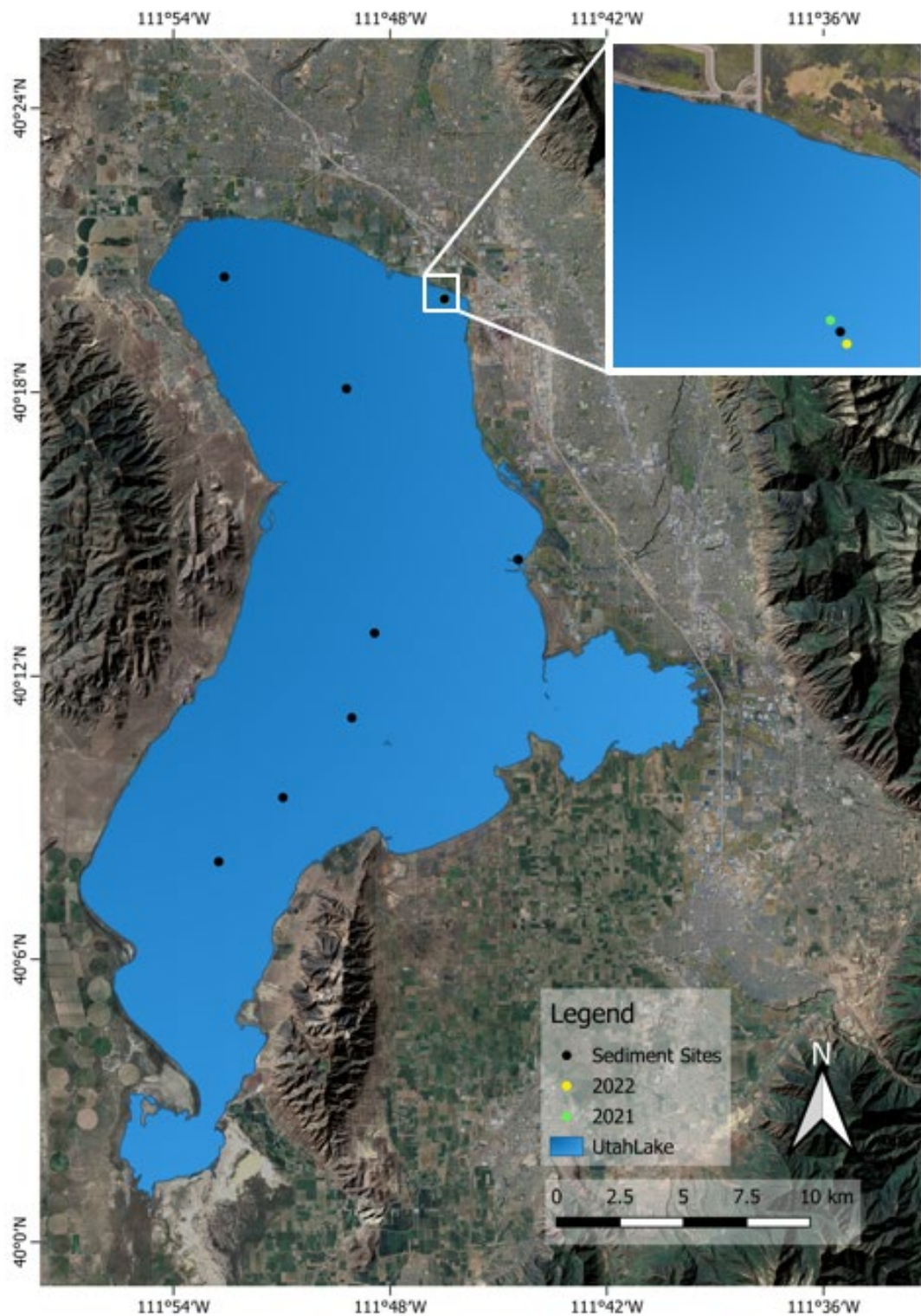


Figure 2-3. Sediment and water sample locations.

2.3 Probe Measurements

We measured pH, ODO, WT, SpC, TU, PhC, and Chl-a in situ using YSI DSS Pro water quality sondes. These probe measurements were taken coincident with the water samples. We calibrated the probes weekly (see Section 2.2). Table 2-1, details the accuracy and resolution for the sonde parameters.

Table 2-1. YSI ProDSS sonde parameter accuracy and resolution [91-95].

Parameter	Accuracy	Resolution
ODO	0 to 20 mg/L: ± 0.1 mg/L or 1%	mg/L
	0 to 50 mg/L: $\pm 8\%$	0.1%
TU	0.3 FNU or $\pm 2\%$	0.1 FNU
SpC	0.1 mS/cm	0.1 mS/cm
WT	$\pm 0.2^\circ\text{C}$	0.1°C
pH	± 0.2 pH units	0.01 pH units
Chl-a	$r^2 = 0.999$ for Rhodamine WT	0.01 $\mu\text{g/L}$
PhC	$r^2 = 0.999$ for Rhodamine WT	0.01 $\mu\text{g/L}$

2.4 Laboratory Analysis Methods

We analyzed water samples for TDS, TSS, and VSS using Standard Methods 2540 C, D, and E. We split each water sample for ICP-OES analysis for dissolved (particles smaller than 0.45-microns) and total concentrations. For dissolved concentrations, we filtered samples using a new 0.45-micron membrane filter. For total concentrations, we performed microwave-assisted acid digestion using a modified EPA 3015A method. Table 2-2 summarizes the methods used for the laboratory analysis of the water samples.

Table 2-2. Lab analytes and methods.

Analyte	Model/Method	Equipment
TDS	Method 2540 C	VWR 1350FM Oven
TSS	Method 2540 D & E	Binder ED53 Oven
VSS	Method 2540 D & E	Thermolyne F62700 Oven
DE Total (digested)	EPA 3015A	Thermo Scientific™ 7400 ICP-OES
DE Dissolved (filtered)	0.45 μm filter	Thermo Scientific™ 7400 ICP-OES

The minimum detection limits (MDL) for our ICP-OES are listed in Table 2-3. The MDLs vary by element but are on the order of a few $\mu\text{g/L}$ or part-per-billion (ppb). The highest MDL for the ICP-OES is for Se at 7.36 ppb or 736 ppm. The lowest MDL is for Ca at 0.02 ppb or 20.0 ppt. The ICP-OES was chosen for sample analysis because it is highly sensitive and allows us to analyze trace elements with the UL water column.

Table 2-3. ICP-OES minimum detection limits (MDLs).

Analyte	Detection Limit ($\mu\text{g/L}$)	Analyte	Detection Limit ($\mu\text{g/L}$)
Aluminum (Al)	1.51	Molybdenum (Mo)	1.11
Arsenic (As)	4.74	Sodium (Na)	1.80
Boron (B)	1.26	Nickel (Ni)	2.29
Barium (Ba)	0.17	Phosphorus (P)	5.66
Calcium (Ca)	0.02	Lead (Pb)	4.50
Cadmium (Cd)	0.19	Sulfur (S)	2.22
Cobalt (Co)	1.16	Selenium (Se)	7.36
Chromium (Cr)	0.85	Silicon (Si)	7.20
Copper (Cu)	2.36	Strontium (Sr)	0.04
Iron (Fe)	0.80	Titanium (Ti)	0.58
Potassium (K)	5.10	Vanadium (V)	0.80
Magnesium (Mg)	0.04	Zinc (Zn)	0.60
Manganese (Mn)	0.21		

2.4.1 Filtration

We used Nyaflo® Membrane Disc Filters with $0.45\mu\text{m}$ pores. It is common practice to consider particles smaller than $0.45\mu\text{m}$ as “dissolved” and larger particles as “suspended” [50, 96]. Dissolved constituents are generally more bioavailable than suspended particles in the water column—suspended particles are typically not bioavailable. For example, clay minerals have a high Al content that is not toxic or generally bioavailable if consumed. Depending on the element, the dissolved and suspended phases can have very different concentrations. For this study, we refer to the samples representing the dissolved concentration in the water column as filtered, and the samples representing the total concentration (which includes both the suspended and dissolved fractions) as unfiltered.

Our quality assurance analyses revealed sample contamination for some analytes caused by the filters we used, with the contaminants listed in Table 2-4. However, we used the same brand of $0.45\mu\text{m}$ filters on all of our filtered samples, and the level of contamination was small. For our analysis, we assume that comparisons and trends based on the sample results are still accurate, even if specific concentration amounts are not.

Table 2-4. Filter contaminants.

Analyte	Analyte
Arsenic (As)	Sodium (Na)
Boron (B)	Sulfur (S)
Potassium (K)	Zinc (Zn)
Magnesium (Mg)	

2.4.2 Sediment Sample Analysis

We analyzed our twelve sediment samples for DE. We followed the EPA 3015A method for microwave-assisted acid digestion before ICP-OES analysis. We converted measured liquid concentrations into mass concentrations (i.e., mg/kg) based on the measured mass of each sample.

3 Data Summary

3.1 Data Nomenclature

For analysis, we abbreviated the labels of the 61 parameters. We labeled results from the ICP-OES detectable elements (DE) with their respective element symbols and the suffix “_U” for unfiltered samples or “_F” for filtered samples. We report all DE analytes in mg/L (ppm for dilute samples). We report TSS, VSS, and TDS data in mg/L. The remaining abbreviations and units are listed in Table 3-1.

Table 3-1. Parameter abbreviations.

Abbreviation	Full Label	Unit
ODO	Optical Dissolved Oxygen	mg/L
TU	Turbidity	NTU
SpC	Specific Conductance	µS/cm
WT	Water Temperature	°C
Chl-a	Chlorophyll-a	µg/L
PhC	Phycocyanin	µg/L
UL_Vol	UL Volume	ac-ft

Units are reported in Table 3-1 as they were recorded by the YSI-Sondes. NTU stands for Nephelometric Turbidity Units and is equivalent to the now-common unit of Formazin Nephelometric Units.

3.2 Data Cleaning

Prior to analysis, we cleaned the dataset to account for measurements below the MDL for each analyte and to impute missing values. For the ICP-OES DE analytes, we replaced concentrations below the MDL (Table 2-3) with half of the MDL. This was done to preserve the detection of the element for analysis.

There were two data points missing for TDS, TSS, and VSS measurements and three data points missing for pH measurements. To preserve the most data possible for analysis, we used the methods listed in Table 3-2 to replace these values.

Two measurements for TDS, TSS, and VSS concentrations were missing within our dataset. One set of TDS, TSS, and VSS measurements were missing for 09/30/2021 and one set for 10/05/2021. We estimated these missing values using coincident probe samples for TDS and correlations with probe turbidity or TSS measurements for missing TSS and VSS data, respectively. We estimated the two missing TSS values using a TSS and turbidity correlation ($R^2 = 0.17$). We estimated the two missing VSS values using a correlation between TSS and VSS ($R^2 = 0.98$).

Three values pH probe measurements were missing for 06/21/2021, 09/21/2021, and 09/23/2021 due to a sensor failure. We replaced the missing pH values by the average of the dataset since pH in UL is relatively stable, ranging from 8.18 to 9.53.

Table 3-2. Data replacement methods.

Parameter	Data Source	Dates Missing	Method
TDS	Laboratory	09/30/2021 10/05/2021	Replaced with coincident TDS probe data
TSS	Laboratory	09/30/2021 10/05/2021	Correlation with Turbidity
VSS	Laboratory	09/30/2021 10/05/2021	Correlation with TSS
pH	Probe	06/21/2021 09/21/2021 09/23/2021	Average of dataset

The final dataset contained 28 samples, each with 61 parameters, collected over the 2021 and 2022 sampling periods for June through October and May through August, respectively. These include 50 DE analytes, 25 filtered and 25 unfiltered; laboratory measured TDS, TSS, and VSS; probe measured ODO, TU, SpC, WT, pH, Chl-a, and PhC; and UL_Vol from the BOR records. A dataset with no missing values was necessary for PCA.

The field sampling summary (Figure 3-1) shows the collection frequency over the 2021 and 2022 sampling seasons. The 2021 sampling season has a gap from late July through late August due to equipment challenges, but increased frequency for September and October. The 2022 sampling season was more consistent during the sampling season but shorter, ending in August except for sediment samples in September and November.

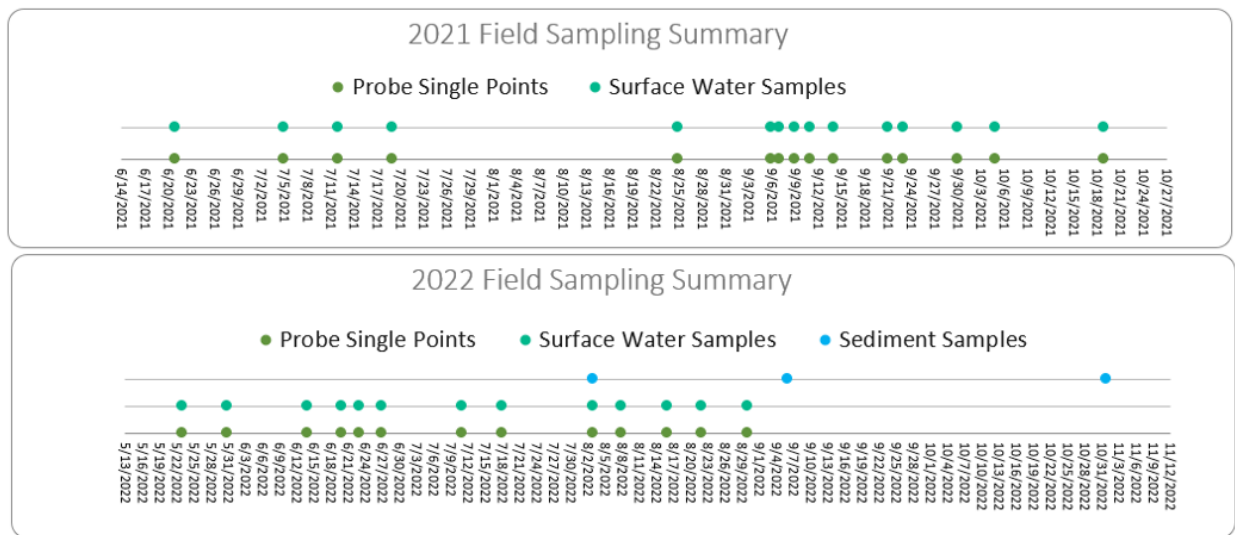


Figure 3-1. Field sampling frequency for 2021 and 2022 sampling seasons.

3.3 MDL Analysis

To identify the impact of replacing DE measurements below the MDLs, we analyzed the frequency of sub-MDL results. Figure 3-2 illustrates the percentage of DE measurements that were above the MDL for both unfiltered and filtered samples. If both the unfiltered and filtered samples measured were above the MDL for every sample, we excluded that DE from the graph for simplification. Forty percent of the DEs had both total and dissolved measurements above the MDL for every sample. These elements were Ba, Ca, K, Mg, Mo, Na, S, Si, Sr, and V.

Less than 20% of filtered or unfiltered samples had Co and Se concentrations above the MDL, and the remainder had concentrations only slightly above the MDL. Co and Se concentrations fluctuate around the MDL. These elements are present in UL, but in trace amounts.

Ti, Cr, Ni, and Pb were above MDLs in less than 20% of filtered samples but were over MDLs in unfiltered samples. These elements are mainly associated with suspended solids, with very low dissolved concentrations. Ti and Cr were above MDLs in 100% of the unfiltered samples, but only 20% of the filtered samples. From this we can infer that these metals are mainly contained in the suspended solids and sediments of UL and are not present as reactive dissolved particles. Unfiltered Ni and Pb were above MDLs about 75% and 45%, respectively. These elements similarly show that they are prevalent within the water column more in the unfiltered than the filtered variant. Knowing the particle size with which elements in the water column are typically associated allows us to better understand how the metals behave within the ecosystem.

One metal, Zn, had more filtered samples over the MDL than unfiltered samples. This indicates that the filters contaminated the samples, as discussed in section 2.2.1. We assume that although the dissolved Zn values are not accurate, the changes and trends in concentration are still relatively correct. As Zn is a vital micronutrient, it is of significant interest for this study.

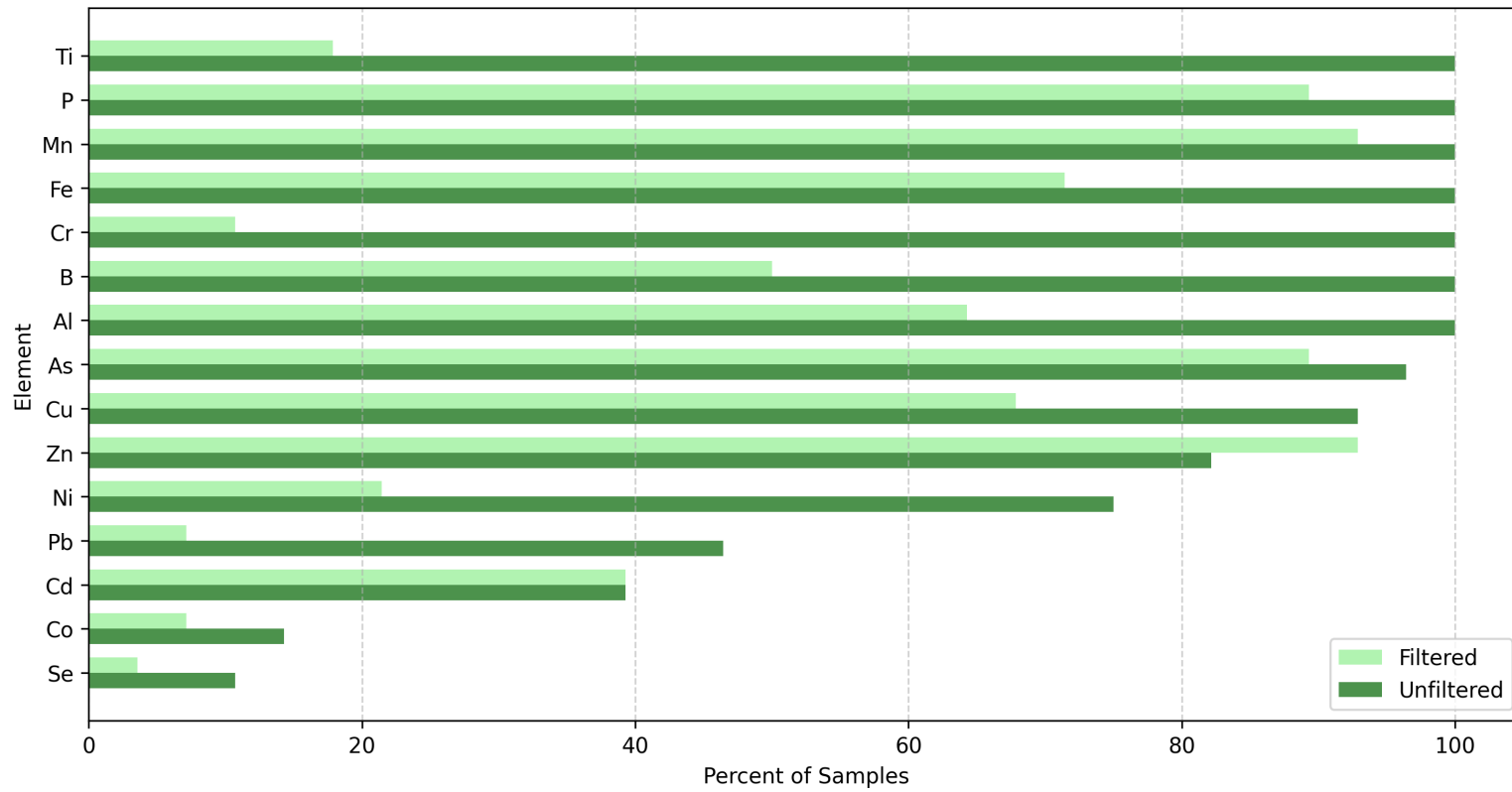


Figure 3-2. Percentage of samples for each ICP-OES analyte with measured concentrations above the MDL. Analytes with 100% detection in both filtered and unfiltered samples excluded.

4 Results

We analyzed the data to determine average percent of elements in sediments, data distributions, and correlations among the analytes. We used PCA and MDS approaches to characterize the relationships among the analytes and how UL conditions changed over time. PCA and MDS analysis provide insight into the relative contribution of each DE over time, and to better understand which analytes behave similarly and under what conditions.

4.1 Sediment Data

We analyzed sediment samples using ICP-OES converted the results to mg/kg. We then averaged the results across sample locations and dates. Table 4-1 contains these average DE concentrations listed in descending order.

Table 4-1. Average concentrations of DEs in UL sediments listed in descending concentration order.

DE	Concentration (mg/kg)	DE	Concentration (mg/kg)
Calcium (Ca)	145,888.3	Zinc (Zn)	145.5
Iron (Fe)	12,495.5	Vanadium (V)	48.2
Magnesium (Mg)	10,417.8	Lead (Pb)	30.5
Aluminum (Al)	8,975.8	Chromium (Cr)	30.0
Sulfur (S)	2,919.2	Boron (B)	24.3
Potassium (K)	2,671.2	Copper (Cu)	19.5
Silicon (Si)	1,752.3	Nickel (Ni)	11.5
Sodium (Na)	857.5	Arsenic (As)	7.3
Phosphorus (P)	715.5	Cobalt (Co)	3.7
Strontium (Sr)	633.7	Molybdenum (Mo)	1.3
Titanium (Ti)	346.0	Cadmium (Cd)	1.2
Manganese (Mn)	278.7	Selenium (Se)	0.0
Barium (Ba)	179.5		

Ca had the highest concentration in the sediments, at approximately 145,888.3 mg/kg (~15% by mass). As UL waters are often at calcite solubility limits, a high calcium concentration is expected. Sediment concentrations of Fe, Mg, and Al ranged from 12,495.5 to 8,975.8 mg/kg, also high as these are common in the lakebed minerals from UL [97]. The rest of the DEs that make up the soil are in Table 4-1.

4.2 CWA-regulated DE Distributions by Year

We analyzed the distributions for the CWA-regulated DEs grouped by year (2021 and 2022) and phase (filtered and unfiltered) as described in section 1.3. We show distributions of Cu, Zn, Ni, Al, Pb, and P as box-and-whisker plots, and present plots for the remaining seven DEs in the appendix (Figure A-1). In these plots the line in the middle of the box is the median concentration, the box ends are the 25th and 75th percentiles, and the whiskers represent 1.5 times the inter-quartile range (1.5xIQR). Outliers, or values outside 1.5xIQR, are shown as dots.

We included lines on each boxplot indicating the most stringent acute (1-hr average) and chronic (4-day average) standards (Table 1-1). All regulations are for dissolved (filtered) concentrations except Al and P, which are based on the total (unfiltered) concentration. We did not follow State-approved methods of analysis. Our findings cannot determine or indicate the impairment status of UL; we include the regulatory criteria to provide context.

In the following figures, the dark blue boxplots are the unfiltered results and the light blue boxplots are the filtered results. The dark green dotted horizontal line represents the chronic standard and the light green line represents the acute standard. In a few cases where the acute and chronic regulations are the same, only the dark green line is visible.

4.2.1 Micronutrients

Cu, Zn, and Ni (Figure 4-1) have both toxic effects from excess concentrations and debilitating ramifications from deficit concentrations as they are micronutrients vital for a healthy ecosystem. Figure 4-1 shows the distribution of Cu, Zn and Ni and standards for these DEs.

Median unfiltered Cu concentrations for both years are above or close to the regulatory criterion, with concentrations more varied in 2021 ($n = 15$ in 2021 and $n = 13$ in 2022). Median filtered Cu concentrations are below the criteria in 2021, but above in 2022.

Although filter contamination slightly increased concentrations of our filtered Zn samples, both filtered and unfiltered concentrations of Zn were well below the most stringent standards. In 2022, the difference between the total and the dissolved Zn was larger than in 2021, but remained low. Filtered Zn concentrations, which are lower than shown because of contamination, are low enough that it is more likely to be limiting or colimiting nutrient for algal growth in UL rather than toxic.

Both total and dissolved Ni concentrations in 2021 and 2022 were well below acute and just below chronic state regulations. Most of the Ni in UL appears to be associated with suspended solids, rather than being dissolved. This matches Figure 3-2 which showed ~70% of the unfiltered Ni measurements were over the MDL, compared to only ~20% of the dissolved measurements. These low Ni concentrations suggest that, like Zn, Ni is more likely to be a limiting or colimiting micronutrient than a toxin in UL.

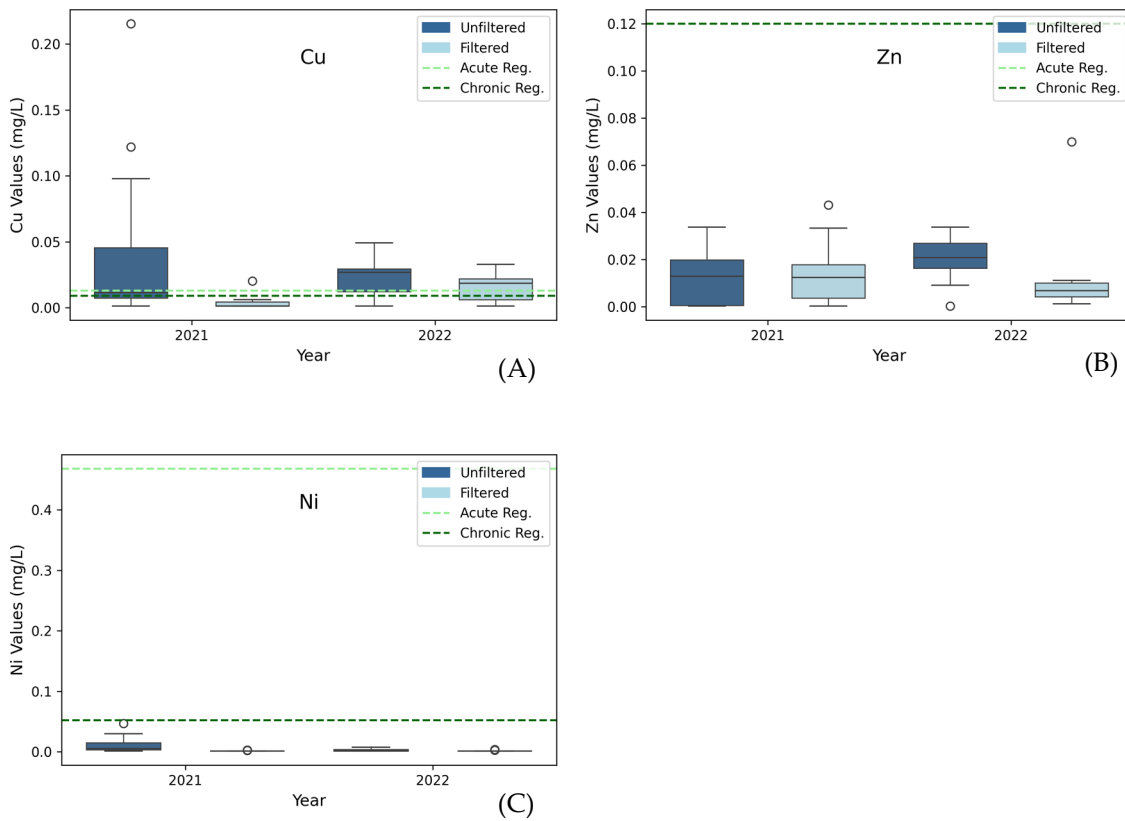


Figure 4-1. Distributions of (A) Cu, (B) Zn, and (C) Ni grouped by year, 2021 and 2022; and phase, unfiltered (dark blue) and filtered (light blue). The plots include reference lines for acute (light green) and chronic (dark green) regulatory values. *Note: when acute and chronic standards are the same only the chronic regulatory values are visible (e.g. Zn).

4.2.2 Aluminum (Al) and Lead (Pb)

Both Al and Pb are nonessential metals that are toxic at high concentrations [59-61, 98]. Al and Pb distributions had median values often near or above their respective state regulations (Figure 4-2).

Unfiltered Al median measurements are above both the acute and chronic criteria. Dissolved Al concentrations, however, are well below the criteria. This indicates Al is associated with suspended solids in the UL water column. We attribute these high total concentrations to suspended clay particles, which makes up a significant portion of the UL sediment (Section 4.1). These unfiltered values represent a total digestion of all suspended solids, including any clay minerals. We did not attempt to follow regulatory methods of analysis, though the current guidelines state “total recoverable”. Our results show dissolved Al concentrations, the phase likely to be bioavailable, are well below levels of concern. While unfiltered concentrations are above levels of concern, they are likely caused by suspended clays. Al and Si ratios (Section 4.1) are consistent with Al

and Mg clay minerals, providing more evidence that high Al concentrations are related to suspended clays.

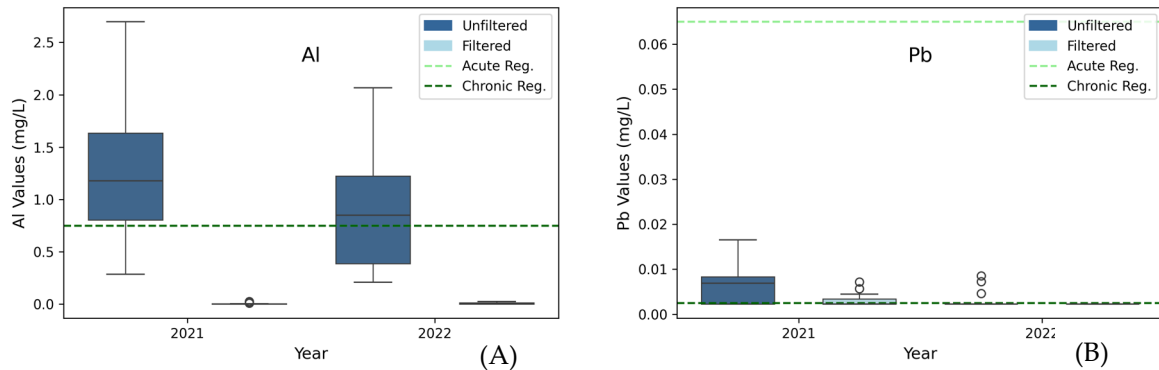


Figure 4-2. Distributions of (A) Al and (B) Pb grouped by year, 2021 and 2022; and phase, unfiltered (dark blue) and filtered (light blue) with reference lines for acute and chronic regulatory levels.

Although our data show that Pb was at or above the regulatory criterion for both filtered and unfiltered samples in both years, this result is an artifact of the MDL for Pb using ICP-OES analysis in conjunction with our data cleaning process. Figure 3-2 showed that Pb is mostly in the form of suspended solids, with just over 50% of our unfiltered samples measuring over the MDL for Pb and less than 10% of the filtered samples measuring over the MDL. The Pb chronic regulation concentrations is half of the ICP-OES MDL for Pb. Since we replaced 90% of measurements that were below the MDL with half the MDL, most of the dissolved Pb measurements are exactly at the chronic regulation. Actual dissolved Pb concentrations could be lower (or higher) than this value. This is a limitation of our study caused by the sensitivity of the ICP-OES. The EPA standard for Pb analysis is ICP-MS.

Both the filtered and unfiltered Pb distributions exhibit large differences between 2021 and 2022, with 2022 exhibiting significantly lower concentrations. We are unaware of any specific cause for this, although it's possible that higher levels of spring runoff in 2021 in comparison to 2022 lead to greater inputs of Pb to the lake in 2021.

4.2.3 Phosphorus (P)

P is a limiting macronutrient in many freshwater lakes [99], but if sufficient P is available, other factors can become the limiting agent. Both total and dissolved P distributions are above the acute and chronic state regulations at the 25th percentile, with the exception of filtered 2022 where the median is above the limits, but the 25th percentile is below (Figure 4-3). UL is listed as impaired due to high P concentrations, and the state has begun the process of developing a total maximum daily load (TMDL) for the lake [100]. Our data support the state data.

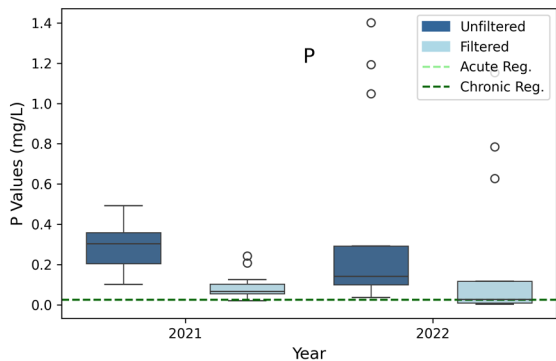


Figure 4-3. Distributions of P grouped by year, 2021 and 2022; and phase, unfiltered (dark blue) and filtered (light blue) with reference lines for acute and chronic regulatory levels.

4.2.4 Barium (Ba)

Ba is a potentially toxic metal that is not currently regulated in Utah [83]. Ba occurs naturally and is also released by industrial processes. It is primarily transported as airborne particles that enter UL through atmospheric deposition [77]. As UL is particularly susceptible to atmospheric deposition, we included a discussion of Ba (section 5.1.5). Figure 4-4 shows the Ba distributions for both filtered and unfiltered measurements. The Ba distributions for 2021 and 2022 sampling seasons are consistent and emphasize the presence of Ba within the UL ecosystem. There is a difference, but not a large one between the unfiltered and filtered distributions. This indicates that a significant portion of Ba is dissolved, with some portion associated with suspended solids. Based on the distributions, about half the Ba in UL is present in the dissolved phase.

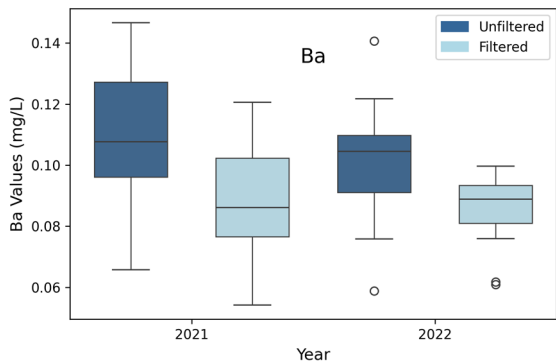


Figure 4-4. Distributions of Ba grouped by year, 2021 and 2022; and phase, unfiltered (dark blue) and filtered (light blue) with reference lines for acute and chronic regulatory levels.

4.3 Data Analysis

We performed an analysis of means (ANOM) and calculated a Pearson correlation coefficient matrix (PCCM) on each analyte. ANOM characterizes and compares the distributions of groups of data, either as months or years in this case, to the population average to determine if the mean of the data in a given month or year is statistically different from the mean of the entire populations. The PCCM is computed pair-wise on each parameter and allows us to visualize the correlation between various parameters.

We expected the populations of the two sampling years to have some variation, as UL experienced very different weather, temperature, and lake volume during 2021 than it did in 2022. We also expected differences in monthly data for some parameters. For example, we expect seasonal differences in TSS, VSS, SPC, and WT in response to the lake heating up in the summer and cooling in the fall along with corresponding volume changes.

For the ANOM analysis, we used an alpha value of 1%, which can be understood to mean that any differences are only likely to occur by chance 1% of the time. The ANOM analysis showed there are statistically significant differences between the two sampling seasons (2021 and 2022) for PhC, As_F, B_F, Cr_U, Cu_F, K_F, Mn_U, Mo_F, Na_F, Si_U, and Si_F, as well as statistically significant differences among data collected in different months for TSS, VSS, TDS, SpC, WT, Al_U, Cd_F, Co_U, K_F, Mg_F, Na_F, P_U, P_F, Si_U, Sr_F, Ti_U, and UL_Vol.

We calculated a Pearson correlation coefficient (PCC) value for all potential pairs of the 61 parameters, with the heatmap of the PCCM shown in Figure 4-5 with PCC values above 0.7 outlined in dark gray. Because of space, correlations are only shown based on the color scale without numerical values depicted. The values on the diagonal are the correlation of a given parameter with itself, and have a PCC of 1, and were not outlined. A total of 54 correlations were strong ($PCC > 0.7$) and are highlighted and listed in Table 4-2.

Strong PCCM correlations indicate parameters change together, likely because they are related to similar processes in the water column. Table 4-2 highlights the patterns seen in the PCCM by listing all the pair-wise correlations with a value greater than 0.7. With the exception of P_U and P_F (0.949 PCC), the unfiltered DEs are strongly correlated with each other, and the filtered DEs are similarly correlated with each other. The strongest PCC values are among the unfiltered DEs, in which various pairs have 31 PCCs with values above 0.7. In comparison, there are 14 PCCs above 0.7 among the filtered DE pairs and 9 non-ICP-OES parameter pairs with PCCs above 0.7.

The highest correlation was between VSS and TSS with a PCC of 0.99. On average the ratio of VSS to TSS was 0.68 within the dataset. This means that, on average, 32% of the suspended solids in UL over our two sampling periods were volatile or organic solids and 68% were inorganic and this ratio was relatively consistent. The only pair with a negative correlation less than -0.7 was the correlation between UL_Vol and TU at -0.726. Which indicates that turbidity is higher when lake levels are lower. This is expected, as when UL is shallow, wind-induced wave action is more likely to disturb the lakebed sediment. As lake volumes increase, the interaction with the sediment decreases because of both depth and the ratio of water to sediment surface area.

Unfiltered Mg_U is strongly correlated to five other unfiltered DE parameters including K_U, S_U, V_U, Sr_U, Na_U, and B_U. Mg_F is strongly correlated to five other filtered DE parameters which are K_F, S_F, V_F, Sr_F, and Na_F. Except for B_U, Mg is strongly correlated with both

unfiltered and filtered K, S, V, Sr, and Na measurements. Mg, S, and K were 9.30% of the total concentration of our measured elements in the sediment samples we collected. This relatively large percentage of Mg, S, and K in the sediments may be why Mg is so strongly correlated with these other DEs in the water column.

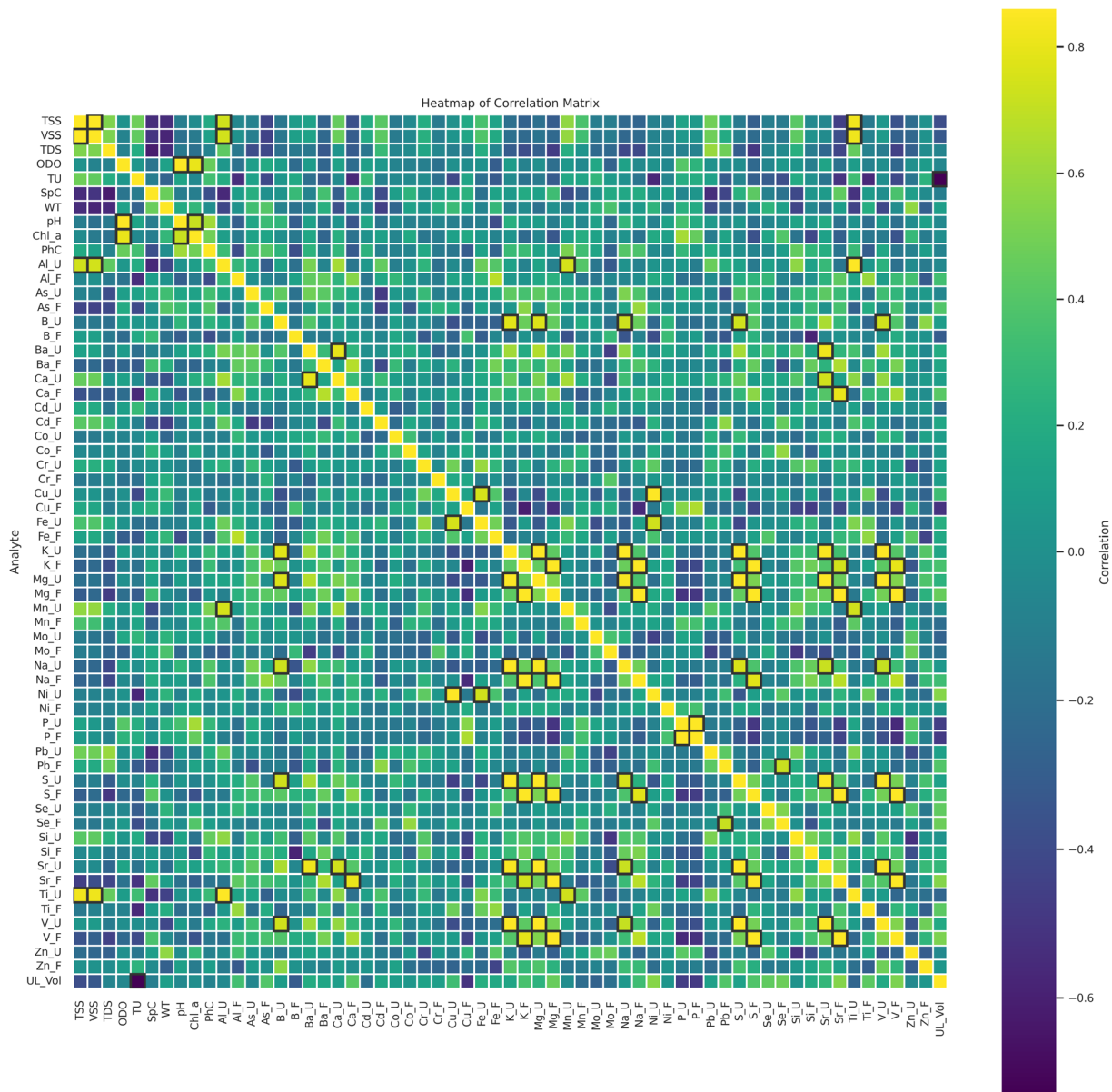


Figure 4-5. Correlation heatmap showing the pair-wise correlation among all 61 parameters. All pairs with correlations greater than 0.7 are outlined in dark gray excluding the correlations of 1 on the diagonal of the square matrix which is the correlation of the parameter with itself and is always 1.

V is another DE that has relatively large PCC values with four other DE pairs, including S, K, Sr, and Mg in both total and dissolved forms. Unfiltered V_U is strongly correlated with unfiltered Na_U.

Another strong correlation is unfiltered Ti_U with both TSS and VSS. This would indicate that unfiltered Ti is correlated with the suspended sediments in UL. The sediment data in Table 4-1 indicates that on average there is about 346.0 mg/kg of Ti in the UL sediments. The relatively small amount of Ti in the sediments and the lack of Ti in the nearby geologic formations could indicate that the Ti present does not come from natural sources, though we would need more data to ascertain this fact [78, 79, 101].

Table 4-2. Pair-wise Pearson correlation coefficients (PCC) for all pairs with values greater than 0.7.

X Parameter	Y Parameter	PCC Value	X Parameter	Y Parameter	PCC Value
VSS	TSS	0.990	Ti_U	TSS	0.823
S_F	Mg_F	0.972	Sr_U	Ba_U	0.820
Na_F	K_F	0.964	Ti_U	VSS	0.816
V_F	S_F	0.956	Chl-a	ODO	0.800
Mg_U	K_U	0.951	Sr_F	Ca_F	0.800
S_U	Mg_U	0.951	V_F	K_F	0.799
P_F	P_U	0.949	Ca_U	Ba_U	0.796
V_F	Mg_F	0.938	K_U	B_U	0.784
Mg_F	K_F	0.931	S_F	Na_F	0.781
Na_U	K_U	0.924	Mg_U	B_U	0.766
V_U	Mg_U	0.924	S_U	Na_U	0.753
Sr_U	Mg_U	0.918	Fe_U	Cu_U	0.752
Ti_U	Al_U	0.916	Mn_U	Al_U	0.750
V_U	S_U	0.911	Al_U	VSS	0.745
Ni_U	Cu_U	0.901	Sr_F	K_F	0.740
V_U	Sr_U	0.897	Sr_U	Ca_U	0.739
V_F	Sr_F	0.885	Ti_U	Mn_U	0.739
Sr_U	S_U	0.884	S_U	B_U	0.737
pH	ODO	0.880	Al_U	TSS	0.737
S_U	K_U	0.874	V_U	B_U	0.736
Sr_F	S_F	0.872	Ni_U	Fe_U	0.735
Sr_F	Mg_F	0.871	Na_U	B_U	0.729
Na_F	Mg_F	0.867	Chl-a	pH	0.718
V_U	K_U	0.861	Se_F	Pb_F	0.718
S_F	K_F	0.858	Sr_U	Na_U	0.714
Sr_U	K_U	0.841	V_U	Na_U	0.709
Na_U	Mg_U	0.840	UL_Vol	TU	-0.726

With respect to biological parameters, there is a strong correlation between Chl-a and ODO. This is unsurprising, as our samples were typically collected mid-day, at the peak of algal photosynthetic activity—more Chl-a indicates more algal biomass, and more algal biomass corresponds to more O₂ being released into the water through photosynthetic respiration by algal cells.

Dissolved oxygen is associated with increased Chl-a during daylight hours. We would expect the inverse relationship between Chl-a and ODO at night but were unable to confirm this because we did not collect data during nighttime hours. pH and Chl-a are also strongly correlated, which we would expect as cellular respiration absorbs carbon dioxide from the water, raising pH.

4.4 Principal Component Analysis (PCA)

We conducted PCA on the full 61-parameter dataset. PCA is a data reduction method that groups parameters that are correlated or behave similarly to each other into groups called principal components (PC). The entire dataset was first standardized using z-scores before the PCA was computed [102].

PCA is a process by which data are linearly transformed from the existing multi-dimensional coordinate system into a new coordinate system. The new coordinate system is chosen so that the coordinates, termed principal components (PCs) capture the largest variation in the data set for each subsequent PC. This general approach is called rotated orthogonal basis functions (ROBF), where the original coordinate system is rotated to a new set of orthogonal coordinates that can be computed as linear weights of the original coordinates (or parameters). The resulting data have the same dimensionality as the original data which can be recovered by the reverse rotation. For data reduction, the minor PCs are excluded when regenerating the data. This results in some loss of accuracy, but doing so greatly simplifies and reduces the parameter space [103]. For our case, we started with 61 parameters and retained 27 PCs.

PCA begins by normalizing the data so that the parameters have a similar magnitude, otherwise those with large magnitudes would overwhelm those with smaller values regardless of variability. We used z-score normalization (also called standard score normalization), using JMP Pro 17®. Following normalization, we computed the eigenvectors and eigenvalues of the covariance matrix to identify the weights and parameters for each of the PCs. For a given PC, the weights for each parameter can be evaluated to ascertain how the various parameters are related and how much each parameter contributes to a given PC. Physical processes can often be attributed to individual PCs based on this type of analysis, though not always.

After performing the PCA, we analyzed the resulting eigenvalues of the matrix to determine how much variability would be captured by each subsequent PC. The eigenvalues of our data in Figure 4-6 (A) show that 19.5% of the variance in the dataset is captured within the first PC, 14% of the variance is captured within the second PC and so on. The first 10 PCs captured 81.9% of the variance within the dataset with the first 14 PCs capturing 90.5%. The scree plot in Figure 4-6 (B) indicates a discernable elbow at 6 PCs. Commonly, the PCs after the elbow are discarded as they contain little information. This eigenvalue analysis shows that if we retained 27 of the 61 PCs, then we will have retained essentially 100% of the variation in the original data. This is a 55.7% reduction in the number of parameters required to describe the system. The remaining PCs can be thought of as representing noise, making it so that we can reconstruct the original data set using these 27 PCs with little loss in information.

Our goal of PCA analysis, however, was not to perform data reduction, but to better characterize and understand the behavior of DEs in UL. This preliminary analysis shows that the detailed 61-dimensional data set can be understood by analyzing a smaller subset of PCs.

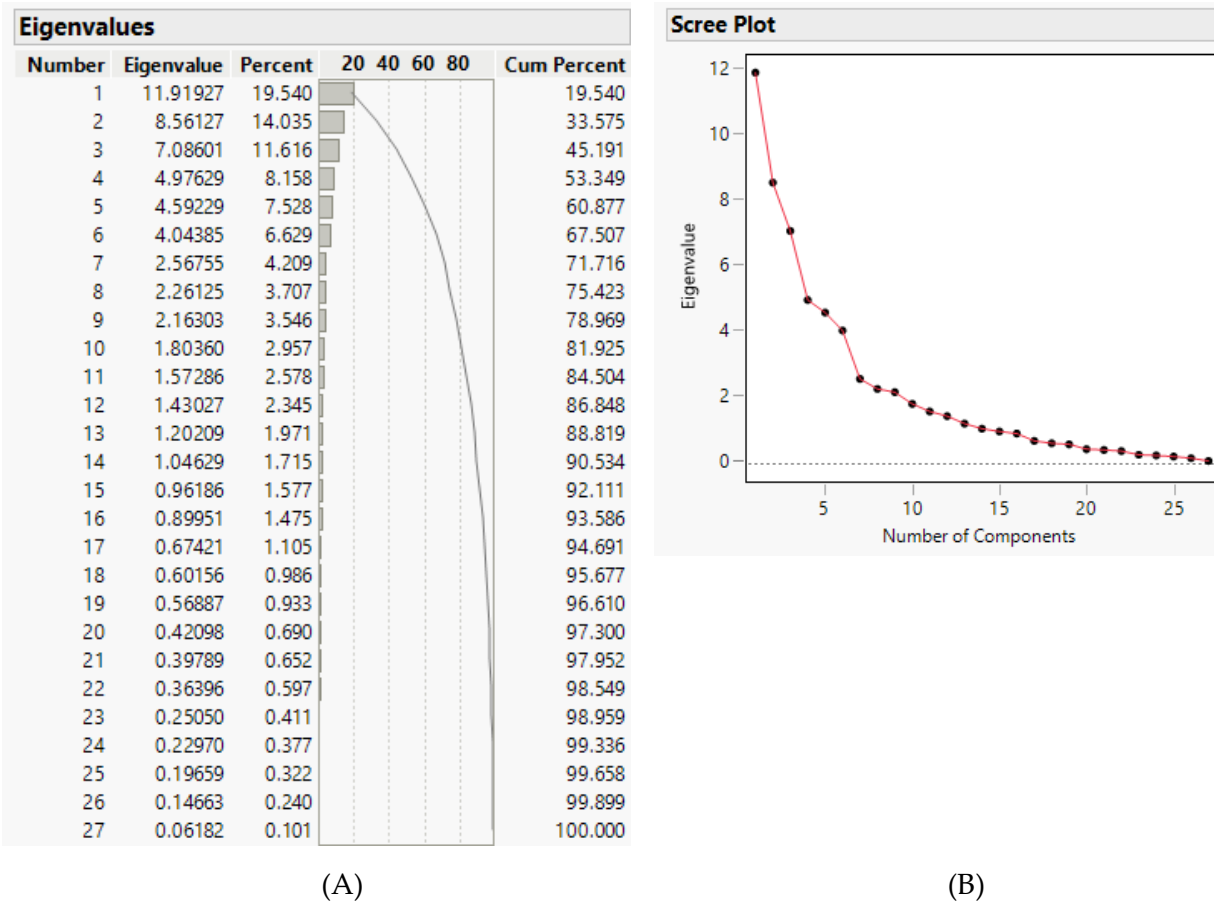


Figure 4-6. (A) The first 27 PCA eigenvalues. (B) PCA Scree Plot of the original 61 parameter dataset.

4.4.1 PCA Loading Matrix

Evaluating the weights or loadings of each parameter in regard to the individual PCs showed us which parameters behave in similar manners. Parameters can contribute significantly to more than one PC, and some parameters contribute to many PCs. The PC loading matrix indicates the weights for each parameter used to generate each PC. Figure 4-7 is a heat map of the formatted loading matrix for the first 20 PCs and Table 4-3 is a PC reference table for the first 5 PCs. To emphasize which parameters are most heavily loaded for each PC, we outlined the parameters with weights greater than 0.5 in a dark gray.

The PC loadings provided intriguing observations, especially in the first 5 PCs which contained 60.87% of the variation within the dataset. We also used these weights to associate physical processes with the various PCs. Rather than looking at pair-wise correlations, as we did in Section 4.3, the parameters here were grouped together based on behavior. Any given parameter is weighted or present in all the PCs, but generally only contributed significantly to a few. Analyzing these PC weights provided insight into how the DEs behave and interact with other parameters. The majority of the heavily weighted parameters in PC 1 are alkali and alkaline earth metals

with the addition of both filtered and unfiltered V and S. B_U and Si_F were also heavily weighted, though they are not alkali or alkaline metals. The main contributors to PC 1 include both the filtered and unfiltered measurements for most of the parameters. The heavily weighted parameters which contribute to PC 1 did not contribute much to any other PCs with the exception of unfiltered K, S, Na, and B, which contributed to PC 3, but with weights below 0.5. We associated PC 1 with the alkali and alkaline earth metals.

Based on the contributing parameters, PC 2 represented the suspended sediments. The main contributors to PC 2 were Ba_U, Al_U, Ti_U, Si_U, Mn_U, Ca_U, Pb_U, PhC, TSS, and VSS. SpC, WT, and Mo_F were inversely weighted. All of the strong positive weights were unfiltered (total) elements that we would expect to be present in the water column as suspended sediments. The unfiltered metals in PC 2 were the trace metals contained within the UL sediments (Table 4-1). The high weighting of VSS and TSS helped us interpret PC 2 as representing the suspended sediments within UL, as these were direct measurements of the amount of suspended solids. The inverse correlations with SpC were also consistent with associating this PC with suspended sediments, as an increase in suspended sediments lead to a decrease in the SpC of the water column.

Table 4-3. PC reference table. Parameters with significant weights (>0.5) within each PC are listed for both positive and negative correlations.

PC	Reference Name	Positively Correlated Parameters	Negatively Correlated Parameters
1	Alkali and Alkaline Earth Metals	Mg_F, V_F, S_F, Sr_F, K_F, Mg_U, Na_F, Sr_U, V_U, K_U, S_U, Na_U, B_U, Ca_F, Ba_F, Si_F, Ba_U	
2	Suspended Sediments	Ba_U, Al_U, Ti_U, TSS, Si_U, VSS, Mn_U, Ca_U, Pb_U, PhC	SpC, Mo_F, WT
3	Transition Metals	Fe_U, Ni_U, Cu_U, Ti_F, Fe_F, Cr_U, UL_Vol	TU, Mo_U
4	Chl-a	Chl-a, WT, P_U, Zn_U, ODO	
5	PhC	Al_F	PhC, As_F

The parameters that played significant roles in PC 3 included the transition metals Fe_U, Fe_F, Cr_U, Ni_U, Cu_U, Ti_F, as well as UL_Vol and its inverse correlations with Mo_U and TU. These transition metals acted in a pattern correlated with UL_Vol. This means that larger lake volumes coincided with larger concentrations of these transition metals. These transition metals may have been influenced by the UL tributaries. In addition to being transition metals, Fe, Ni, and Cu are also micronutrients.

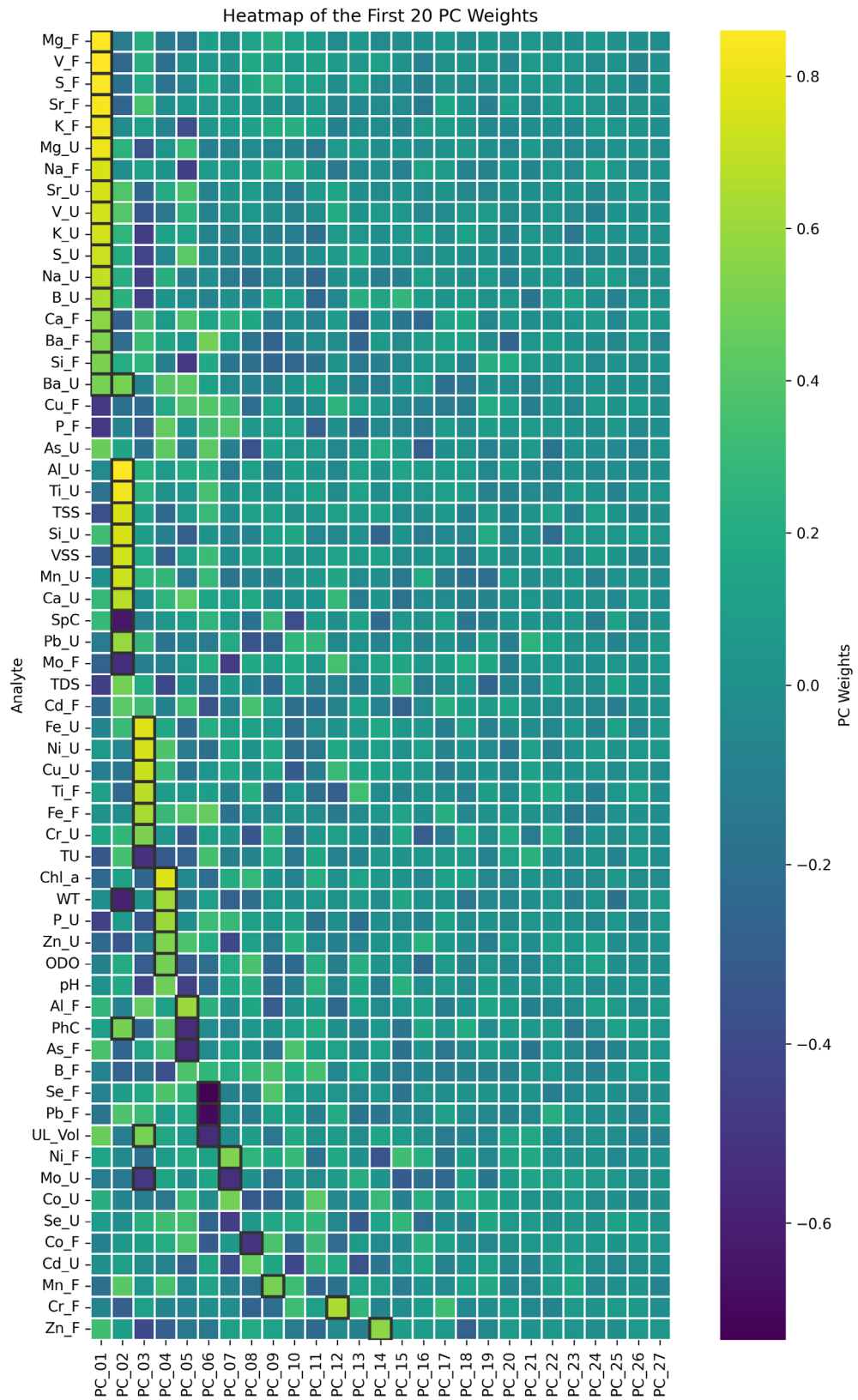


Figure 4-7. PC loading matrix. Weights above 0.5 are outlined in dark gray.

The significant parameters which contributed to PC 4 included Chl-a, WT, P_U, Zn_U, and ODO. The impacts of WT on Chl-a are well known, with warmer waters resulting in more Chl-a because of phytoplankton growth. PC 4 indicated that unfiltered P correlated with Chl-a more than filtered P. Filtered P is available for growth, but unfiltered is probably attached to suspended materials including biomass. This supports the hypothesis of UL being light-limited rather than P limited. The correlation of P_U with Chl-a is likely a result of P contained in phytoplankton cells. The fact that dissolved P was not correlated with the phytoplankton growth (estimated with the Chl-a) would indicate that phytoplankton growth is not responding directly to bioavailable P concentrations—meaning it is not a limiting factor in the UL water column. P_U played a significant role in PC 4, with a weight of 0.61, and P_F did not play as a significant role in this PC but had a weight of 0.45 which was just below the “significant” threshold. As Zn is a vital micronutrient for algal growth [40-42], the Zn_U correlation with Chl-a is likely a consequence of our digestion method capturing Zn within the algal cells. ODO is generated by phytoplankton growth in sunlight and we expected it to have a correlation with Chl-a.

In PC 5, PhC was inversely correlated with Al_F and positively correlated with As_F. These correlations were likely due to the annual cyclical nature of each of these parameters. PhC increases in the summer and decreases in the fall after the growing season, which happened to coincide with the seasonal trend we observed in As concentrations (Figure 4-8). There is no likely physical reason why they were correlated, rather they were both governed by seasonal variations. As likely increased in late summer because groundwater inflows with higher concentrations of As become a larger portion of lake inflows at that time of year [104, 105].

Despite often being connected with Chl-a in the literature, we found that PhC was not actually correlated with Chl-a concentrations in UL. Nor was it correlated with P (total or dissolved). PhC is an important consideration in HAB mitigation efforts as it indicates the presence of potentially toxin-producing cyanobacteria. It is well known that cyanobacteria and phytoplankton cell counts are not well correlated, but in UL it would appear that cyanobacteria, like phytoplankton, also do not respond directly to P concentrations, which is contrary to findings on less turbid lakes where nutrient concentrations are a primary driver of both planktonic and cyanobacterial HABs. As cyanobacteria is of such a significant management concern, it would be beneficial to further investigate the complex relationships between phycocyanin and nutrient concentrations, water temperature, and turbidity in UL.

Although our results have indicated that it may not be a primary driver of algal blooms, P is still a parameter of great interest in UL due to the regulatory climate surrounding it. A strong P_U and P_F correlation was viewed in the PCCM (Figure 4-5), indicating that filtered and unfiltered P are generally transported together in the UL water column. We further investigated P contributions to other PCs and found that P_F and P_U had similar weights in PC 1, -0.479 and -0.447 respectively, and in PC 3, -0.306 and -0.337 respectively. The significant difference in weights was most prominent in PC 4 with P_F with a weight of 0.453 and P_U with a weight of 0.609. Considering the relatively even weights in PC 1 and PC 3 for P_U and P_F the weight difference in PC 4 would indicate that the lake may be limited by some factor other than P such as light or micronutrients.

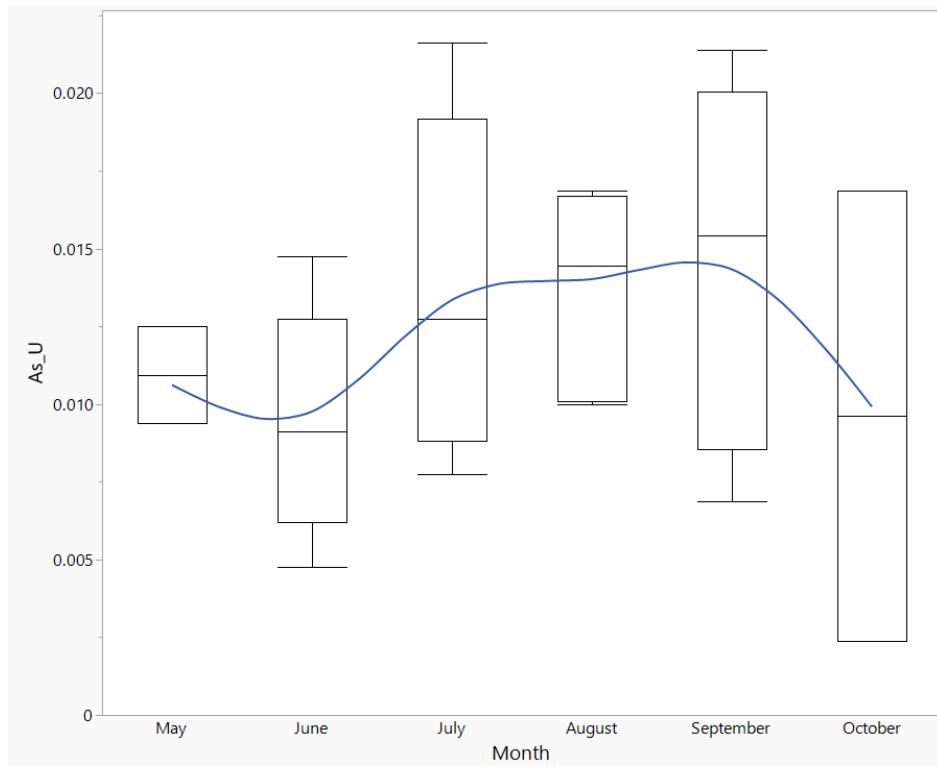


Figure 4-8. As_U cyclical trend.

4.4.2 Variation of PCs over Time

PCs can be plotted and studied as individual parameters with different PCs representing different processes or groups. Figure 4-9 depicts how PCs 1, 2, and 5 changed throughout the sampling season, with values interpolated using the pandas python library with the PCHIP spline interpolation method [106].

PCs 1, 2, and 5 (representative of the alkali and alkaline earth metals, suspended sediments, and PhC, respectively) had similar trends throughout both sampling seasons. In 2021, there was a decline in all three PCs in early to mid-July as well as in early to mid-September. In 2022, the three PCs declined earlier in late June. The second decline was not visible in 2022, possibly due to the shortened sampling season.

PCs 3 and 4 (representing the transition metals and Chl-a grouping respectively) are shown in Figure 4-10. These two PCs behaved opposite of each other. In 2021, there was an opposing spike in early to mid-July and there was a series of three smaller opposing spikes throughout the month of September. In 2022, The initial opposing spike occurred in mid-June and another spike occurred in early August. The relationship between these PCs suggests that transition metals and the Chl-a grouping spikes regularly differed from each other, experiencing significant changes in June/July as well as August/September, which corresponded with early diatom blooms and later green or blue/green algae blooms. Fe and Cu, significant parameters in PC 3, are vital micronutrients for algal growth [40]. When there was an increase in algal growth, there was a

corresponding decrease in dissolved Fe and Cu, which we assumed this was due to algae up taking those micronutrients for growth [40].

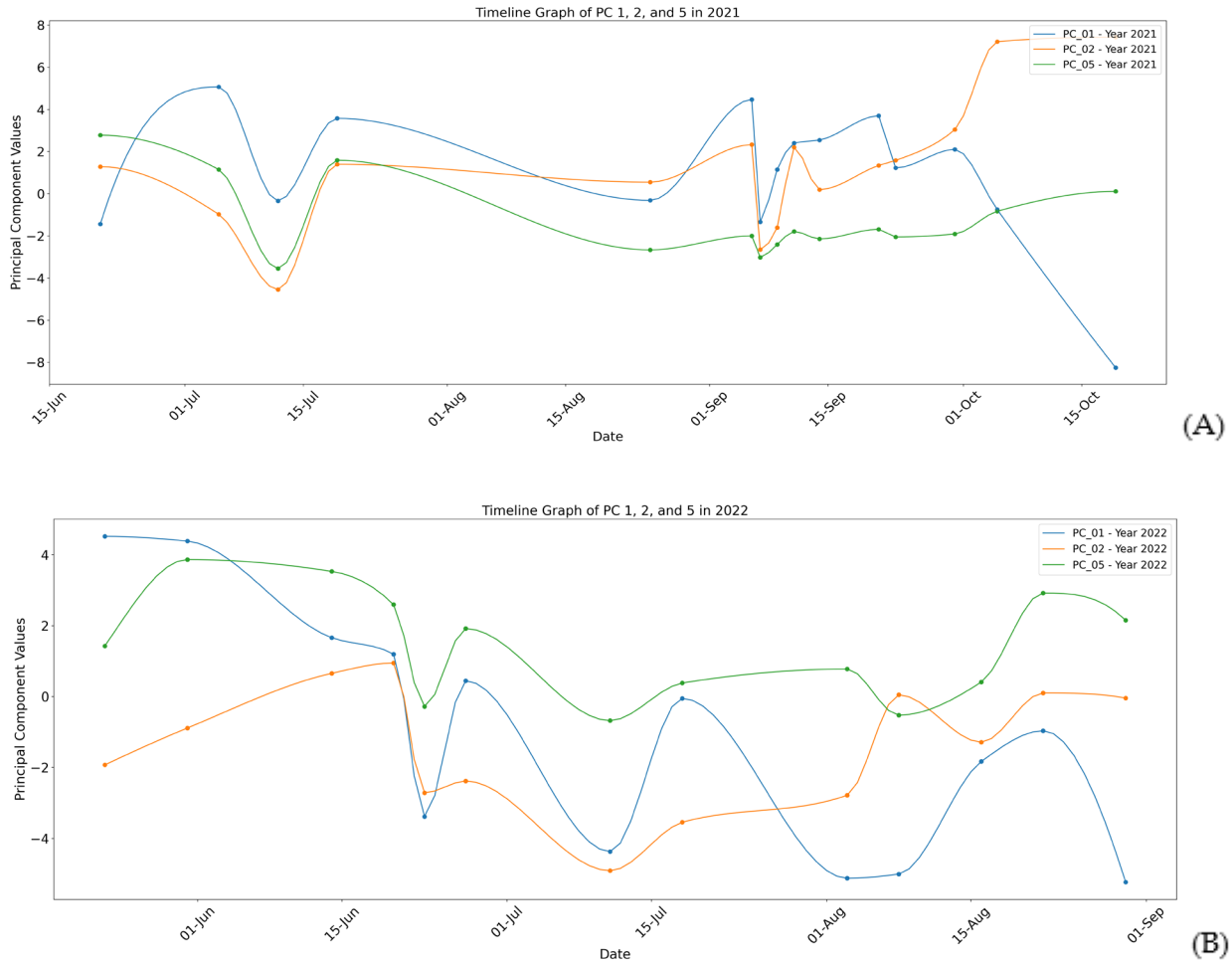


Figure 4-9. PC 1, 2, and 5 values through time for the 2021 (A) and 2022 (B) sampling seasons.

For management strategies seeking to mitigate HABs in UL, it is important to consider the necessary macro and micronutrients that might limit or colimit algal growth in addition to nutrients. These PCs highlight that PhC shows similar peaks to that of the alkali and alkaline earth metals and suspended sediments. With PhC as an estimate of cyanobacteria, correlations such as these can inform effective further research on UL to mitigate HABs.

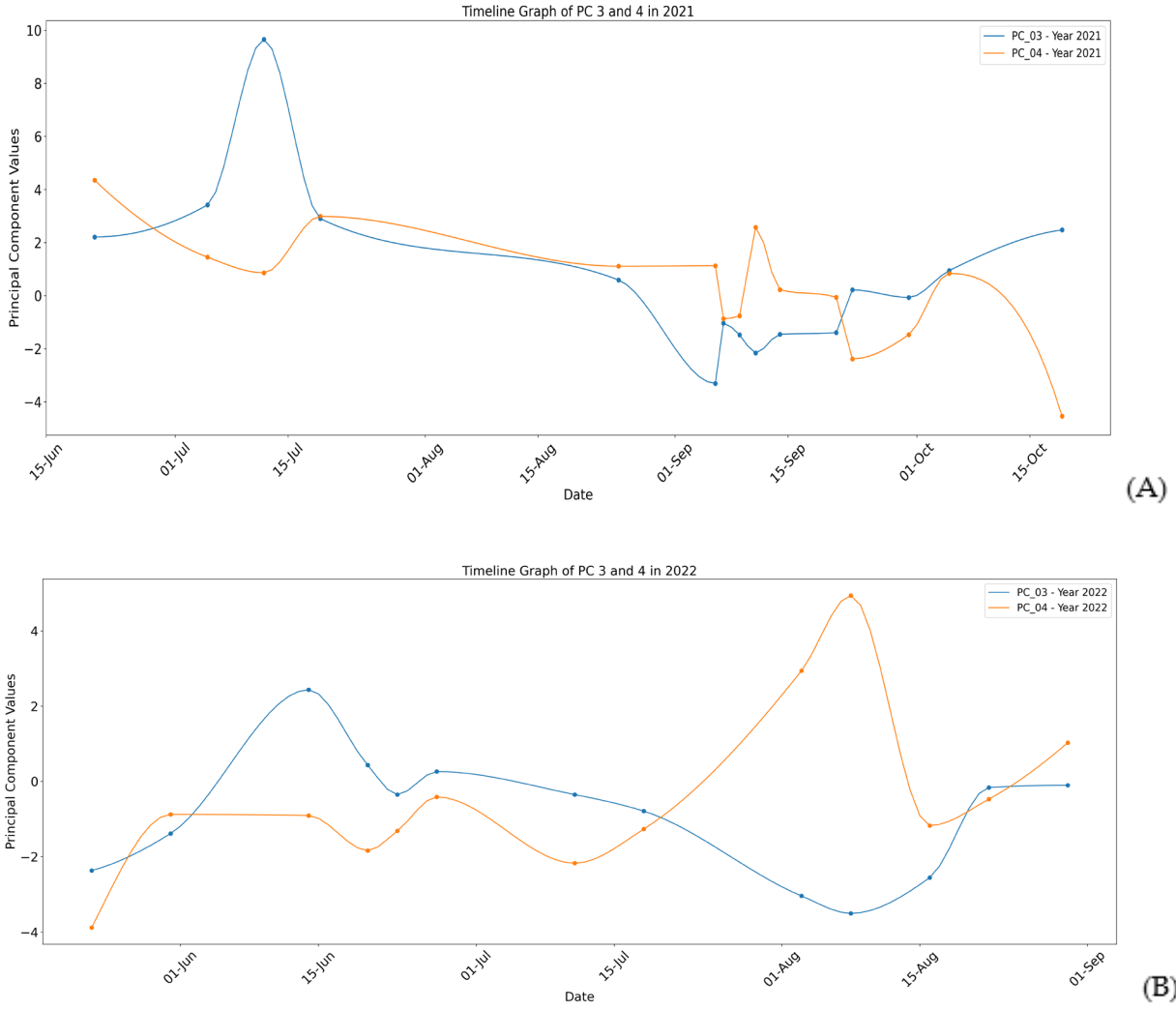


Figure 4-10. PC 3 and 4 timelines for the 2021 (A) and 2022 (B) sampling seasons.

4.5 Multidimensional scaling (MDS)

We conducted an MDS analysis using JMP Pro 17®. MDS is a statistical nonlinear dimensional reduction technique used to visualize the distance between samples in high-dimensional space. This technique reduces the complexity of a dataset by considering the distance in high-dimensional space between two datapoints MDS then finds a mapping in and visually displays the distance on a two-dimensional graph [17, 107, 108]. For our analysis, we used Euclidean distance, but other distance measures such as spectral angle, which is insensitive to dilution, could be used [109].

We computed the Euclidean distance, or PCC matrix, using all 61 parameters. The distance between any two points is the PCC values discussed before. MDS allows us to understand how all the points relate to each other, as opposed to just individual pairs. Any points on the MDS plot

that are near each other in MDS space are similarly close to each other in 61-dimensional space and indicates that the parameters are similar to each other.

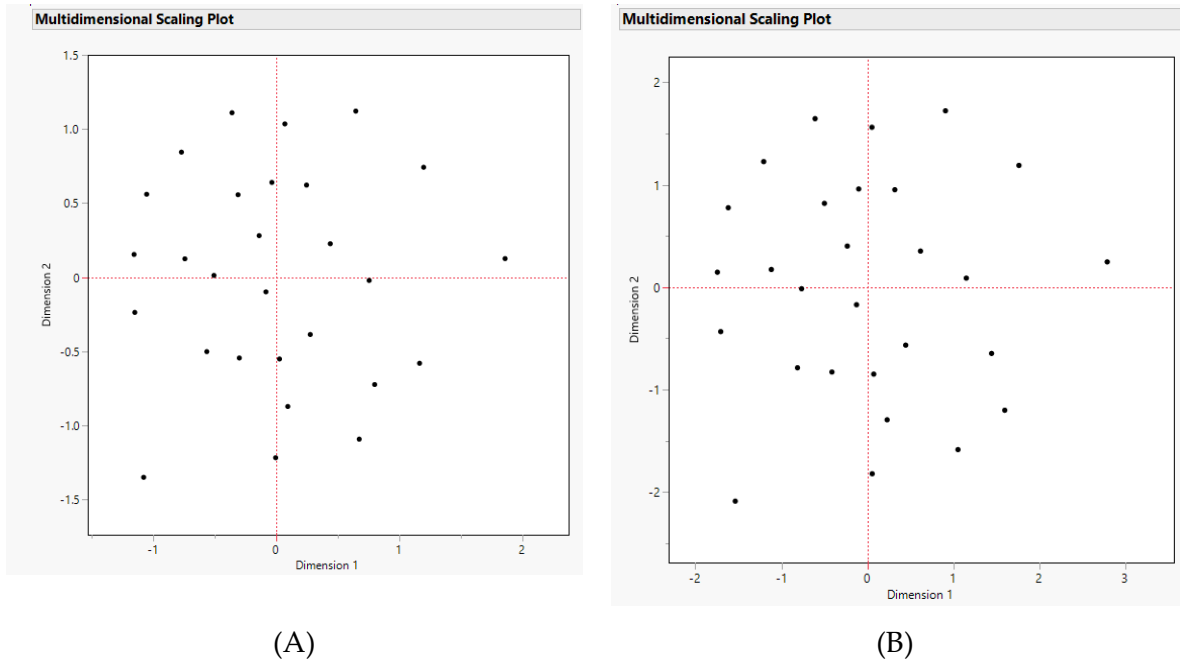


Figure 4-11. (A) Euclidean MDS scaling plot for the 61-parameter data using z-score standardization. (B) Euclidean MDS scaling plot for the 27 PCs. Each plot shows all 28 samples.

For this study we conducted an MDS analysis on two different datasets; the original data using a z-scored standardization and 61 parameters, and the PCs dataset with 27 parameters. We did not need to standardize the PC data as they were already scaled to a similar range. The MDS plots from both data sets resulted in similar groupings and findings. MDS plots can be flipped or rotated after making slight changes to the data or using different data sets, as the MDS coordinates are not physically meaningful. For the MDS plots are shown in Figure 4-11, we flipped the MDS plot generated using PC data both horizontally and vertically, and found that the two plots were almost identical.

We used Shepherd Diagrams to determine how well the MDS distances matched the original distances. In addition to the diagrams, this analysis computes stress and r-squared values. The Shepherd Diagram is computed by plotting the pair-wise distance between every point in both high-dimensional and MDS space. If the resulting distance pairs plot on a straight line, the MDS mapping is a good fit. The stress values range from 0 to 1 with lower numbers signifying a closer fit [110].

For our MDS analysis, the Shepherd Diagram stress and r-squared values are reported in Table 4-4. Both the original data and the PC data had similar stress and r-squared values, both of which showed that the MDS mapping was a good representation of the distance between the data points or samples.

The almost identical MDS scaling plot (Figure 4-11) and shepherd diagram indicators (Table 4-4) result from both the original full standardized data (61 parameter) and the reduced (27 parameter) PC data, indicating that the PCA groupings were able to capture the variation within

the dataset well. The 27 PC parameters describe the relationships among the parameters as well as the full 61 parameter data set. In other words, one use of the MDS scaling plots was a data validation tool for the PCA groupings.

Table 4-4. Shepherd diagram fit details for the z-score standardized and PC datasets.

Fit Detail	Z-Scored Standardized	PC Dataset
Stress	0.2766	0.2767
r-squared	0.6703	0.6702

To analyze the MDS plots, we colored each point based on the month and year the sample was collected (Figure 4-12). Each sampling year grouped together with the 2021 data points coalesced towards the bottom half of the graph and the 2022 points toward the top half of the graph. This indicates that the samples within each year were similar and that different trends were observed in the different years. The water levels between years, in addition to other factors such as weather, likely drove the differences observed between years.

The data were grouped by month in the MDS plots (Figure 4-12), showing that samples changed with time. We outlined the most prominent monthly groupings in the black, yellow, and blue ovals in Figure 4-12. The black oval includes samples taken in May and June. The yellow oval contains the samples taken in August, and the blue oval comprises the samples taken in September. These groups indicate seasonal changes within UL that correspond to spring (May and June), summer (August), and fall (September)). The samples taken in July and October are not close to each other, which indicates transition periods between the seasons. In the case of October, there may just be a lack of data points to discern a pattern. There were only a few October data points acquired for the 2021 sampling season and none for the 2022 sampling season.

We also evaluated the MDS plots by coloring the data by TU, WT, pH, Chl-a, PhC, and SpC. However, we did not discern any patterns or groups with these plots.

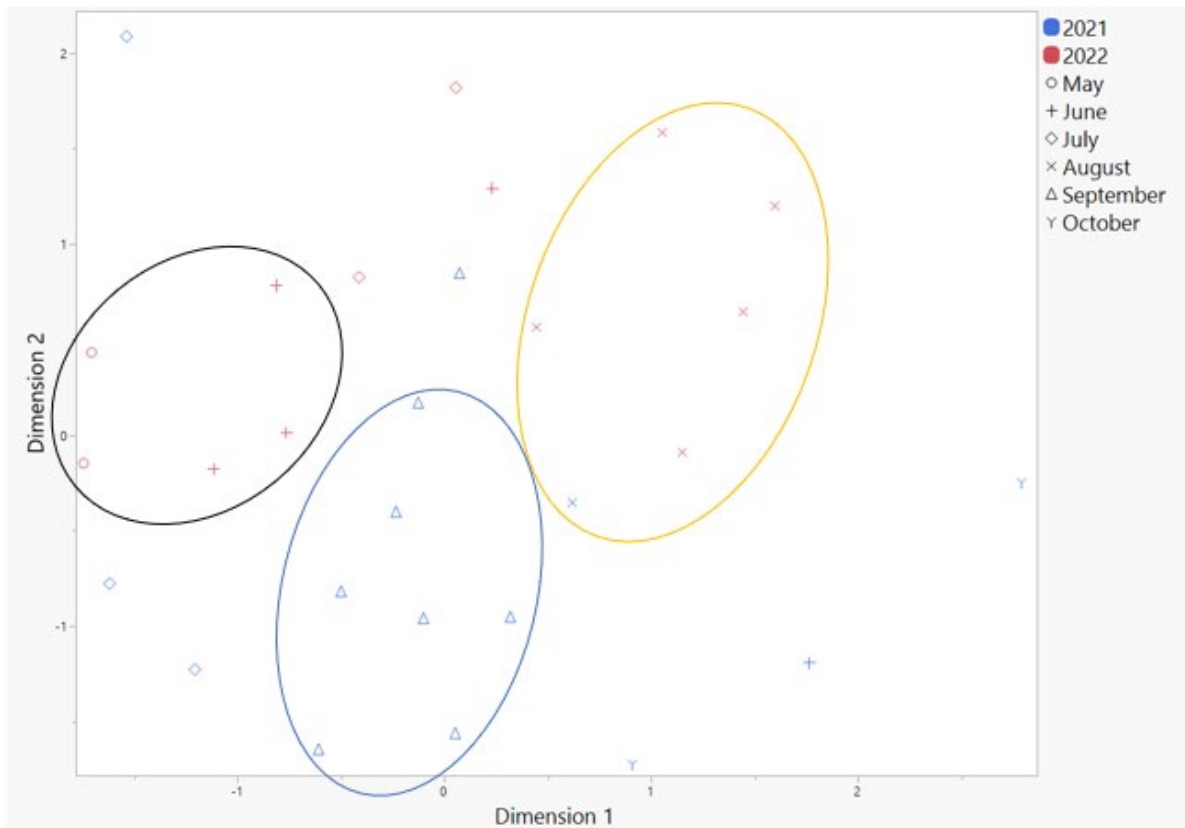


Figure 4-12. MDS data groupings for the z-score dataset.

5 Discussion

5.1 *Elements*

We have chosen to highlight five of the ICP-OES elements we assessed from the UL water column that were either close to or over the most stringent applicable standards or exhibited other interesting characteristics. Here we synthesize our findings for these elements.

5.1.1 Copper (Cu) and Nickel (Ni)

Cu and Ni are transition metals and micronutrients. For both the total and dissolved measurements, over 70% of the water samples contained concentrations of Cu over the MDL (Figure 3-2). Ni is more frequently present in the unfiltered samples than filtered, with over 70% of unfiltered and just over 20% of the samples measuring above the MDL for Ni.

When we compare Cu concentrations to regulatory levels, our data indicate that Cu_F in the 2021 sampling season was below regulatory criteria, but exceeded it during the 2022 sampling season (Figure 4-1 (A)). The state regulations for Cu are only applicable to the filtered samples, but for context, Cu_U was above regulations for both sampling seasons. Both Ni_U and Ni_F were well below the regulatory concentration levels for both acute and chronic conditions (Figure 4-1 (C)). For reference, the UL sediments on average contain 19.5 and 11.5 mg/kg of Cu and Ni, respectively (Table 4-1).

The elevated levels of Cu we observed may be related to the use of copper sulfate-based algaecide which the State began using to treat intense algal blooms in marinas in 2020 [111, 112]. Our study location is located less than 1 km (0.6 miles) from Lindon Marina and 2 km (1.25 miles) from American Fork Marina. The Utah Department of Environmental Quality (UDEQ) released an interim report on UL Marina HAB treatments in which they found that “copper concentration increased considerably” in the days following treatment but returned to below toxic levels within a week [111]. The higher concentrations of dissolved Cu in 2022 relative to 2021 may also be due to the lower lake levels during the 2022 sampling season. The lake had on average about 49 million cubic meters (39,700 ac-ft) less volume in 2022 than in 2021 due to the low snowpack of the preceding spring, which may have increased the water column concentrations of several elements

[90]. Although the use of algaecide and low lake levels are one potential cause of the elevated levels of Cu observed in both years, they may not be the drivers. Additional research is needed to identify and characterize the source and behavior of these metals. This is important, as our results show that levels of dissolved Cu in the lake could be approaching harmful concentrations.

Correlation analysis found that Cu_U is strongly correlated with Ni_U and Fe_U, with PCCs of 0.901 and 0.752 respectively. Ni_U also had a strong correlation with Fe_U, with a PCC of 0.735 (Table 4-2). These metals are all transition metals, with Ni being another micronutrient. Within the PCA analysis, Cu_U and Ni_U played a significant role in PC 3 in addition to Fe_U, Ni_U, Ti_U, Fe_F, Cr_U, and UL_Vol. The grouping of these transition metals within the PCA means that these metals act similarly within the water column.

The PC timelines for PC 3 and 4 showed consistently opposing peaks (Figure 4-10) between these transition metals and the Chl-a-related parameters (WT, P_U, Zn_U, ODO, and pH). This trend is very clear in both of the sampling periods, with spikes occurring at the beginning and ending of the sampling season. We have no explanation for this strong negative correlation, but a better understanding of this could aid in developing HAB management strategies for UL.

Our yearly distribution plots indicated that dissolved Cu may be increasing in the lake. The Cu-based algaecides are not the only source of Cu in UL, but their use warrants additional study. Ni likewise warrants additional study as it is strongly correlated with Cu and is grouped with the transition metals that consistently decrease when Chl-a increases or increase when Chl-a decreases. This correlation may indicate that algaecide applications are not the drivers for the high Cu concentrations. The relationship among the transition metals is not fully understood but should be further studied as their negative correlation with Chl-a could lead to insights for effective management of HABs in UL.

5.1.2 Zinc (Zn)

Zn is toxic at high concentrations but can impair the health of an ecosystem at deficient quantities. Our data suggest that Zn is present in both the water column and lakebed sediments, with more than 80% of both the filtered and unfiltered samples measuring above the MDL for Zn (Figure 3-2) and Zn having an average concentration of 145.5 mg/kg in the sediments in UL (Table 4-1).

Neither the filtered nor unfiltered Zn measurements showed a PCC over 0.7 with any other parameter. PCA, however, grouped Zn_U with Chl-a. In other words, the PCA found that Zn_U and Chl-a (in addition to WT, P_U, ODO, and pH) behaved similarly throughout the course of the two sampling seasons. However, only unfiltered Zn, not dissolved Zn, is grouped with Chl-a. This may indicate that the measured Zn was the Zn present inside algal cells. This underscores Zn as a vital micronutrient for algae in Utah Lake.

Interestingly, Zn_U did not behave similarly to the other micronutrients and transition metals in PC 3. Our data and analyses would suggest that Zn plays a different role than the other micronutrients in algal growth, though we do not understand the processes. Zn concentrations were well below acute and chronic regulatory levels for both unfiltered and filtered samples.

Further research into Zn as a potential colimiting nutrient could be beneficial to developing a better understanding of algal growth in UL.

5.1.3 Aluminum (Al)

The average concentration of Al in the sediment is 8,975.8 mg/kg or almost 0.9% by mass. This concentration of Al is an order of magnitude higher than the amount of Zn and two orders of magnitude greater than the concentrations of Cu and Ni in the sediments. Over 100% and 60% of the unfiltered and filtered Al measurements, respectively, were above the Al MDL (Figure 3-2).

Unfiltered Al was strongly correlated with Ti_U, Mn_U, VSS and TSS with PCCs of 0.916, 0.750, 0.745, and 0.737 respectively. The PCA grouped Al in PC 2 with these same parameters in addition to Si_U, Ca_U, Pb_U, Ba_U, and PhC. The groupings from the PCA suggest that Al is correlated with the suspended solids and sediments of UL.

State water quality regulations require measurements of dissolved (filtered) concentrations of elements except for Al. For Al, the state regulations require “total recoverable” concentrations, which we took to mean unfiltered samples. Figure 4-2 (A) shows that the unfiltered Al samples, when measured using full-digestion and ICP-OES, exceeds the regulatory criteria in both the 2021 and 2022 sampling seasons for both the acute and chronic regulations. The filtered samples, however, are well below the state regulations for both sampling periods. With the presence of soft clay in the lakebed sediments, we believe that most of the Al present in the unfiltered samples is from the clay minerals suspended in UL. Al in the form of clay minerals is nontoxic to the environment and are not of concern.

5.1.4 Phosphorus (P)

P is a vital macronutrient that is a limiting nutrient for algal growth in most freshwater lakes [99]. The Delle Phosphatic and Meade Peak geologic formations within the UL watershed contribute large amounts of P to the lake through natural weathering [20, 78, 79]. The average P within the UL sediment is 715.5 mg/kg (Table 4-1), with literature values in the same range [20, 113]. UL also received P from non-point sources such as agricultural runoff and atmospheric deposition and point sources such as wastewater effluent from the seven WWTPs surrounding UL [16-18, 68]. UL is out of compliance for P and the state has completed a TMDL study [100] to develop management strategies [20]. Our data agree and show P concentrations in both the filtered and unfiltered samples above the regulatory levels. The MDL analysis further emphasizes the presence of P with over 80% of the filtered and all of the unfiltered samples over the MDL (Figure 3-2).

In the correlation analysis, our data show that P_F and P_U are strongly correlated with a PCC of 0.949. There were, however, no strong correlations of P (filtered or unfiltered) with any other parameters. The strong correlation between unfiltered and filtered P would indicate that when there are more suspended sediments within the water column, the P_F increases. This suggests that dissolved P concentrations are governed by a sorption process which keeps sorbed (unfiltered) and dissolved (filtered) P in a constant ratio [114].

The PCA placed P_U in PC 4 with the Chl-a parameters. P_F was not significantly weighted in any of the PCs. This was surprising as P_U and P_F had such a strong correlation in the PCCM. The PC weights of P_F are spread among PCs 1, 3, and 4 with respective weights of -0.480, -0.306, and 0.453. The weights of P_U were also spread out among PCs 1, 3, and 4 with respective weights of -0.447, -0.337, and 0.610.

The fact that dissolved P was not correlated with the phytoplankton growth (estimated with the Chl-a) would indicate that phytoplankton growth is not responding directly to bioavailable P

concentrations—meaning it is not a limiting factor in the UL water column. This analysis indicated that P concentrations, both filtered and unfiltered, are independent of other processes. This is consistent with P acting in a sorption-based system, where water column concentrations are in equilibrium with the sediments which have high P-concentrations of geologic origin [114].

5.1.5 Barium (Ba)

Ba is a potentially toxic metal that is not currently regulated in UL but is present in the lake. The U.S. EPA released a factsheet on Ba [115] in which they state that between the years of 1987 and 1993 1,500 lbs of Ba were estimated to have been released into the waters of Utah. The MDL analysis (Figure 3-2) revealed that Ba measurements for both unfiltered and filtered samples were over MDL 100% of the time. Sediment samples (Table 4-1) suggest that on average there is 179.5 mg/kg in the UL sediments. The Ba boxplot (Figure 4-4) shows that the median unfiltered and filtered samples for Ba are about the same in both the 2021 and 2022 sampling seasons.

Short-term health effects of Ba include gastrointestinal disturbances and muscular weakness and long-term effects include high blood pressure for levels above the maximum contaminant limit (MCL) [115]. The U.S. EPA MCL for Ba is 2 mg/L for drinking water [115, 116]. Within the state of Utah, Ba is only regulated for the designated use of 1C or “Domestic Source” at a maximum dissolved limit of 1 mg/L [83]. The Ba distribution plot (Figure 4-4) shows that both the unfiltered and filtered measurements are well below the EPA MCL of 2 mg/L for drinking water and the 1 mg/L Utah 1C regulation for domestic source water.

Statistical analysis showed a strong correlation of Ba_U with Sr_U and Ca_U with PCCs of 0.820 and 0.796 respectively (Figure 4-5, Table 4-2). Ba_U and Ba_F were significantly weighted in PC 1 with the other alkali and alkaline earth metals (Figure 4-7). The PC timeline for PCs 1, 2, and 5, (Figure 4-9) show that the alkali and alkaline earth metals behave similarly to the suspended sediments and the PhC during the 2021 and most of the 2022 sampling periods.

5.2 Chlorophyll-a (Chl-a) and Phycocyanin (PhC)

Chl-a and PhC are of great interest for UL as they are index parameters for HABs in the lake. In our PCC analysis we found a strong PCC between Chl-a, ODO, and with pH, which have respective PCCs of 0.80 and 0.72. PhC had no strong correlations with any other parameters. The PCA analysis, interestingly, found strong behavioral trends for both Chl-a and PhC but did not weight them heavily within the same PC. PhC was grouped with the suspended sediments within PC 2 (Al_U, Ti_U, TSS, Si_U, VSS, Mn_U, Ca_U, and Pb_U) and Chl-a was grouped with PC 4 (WT, P_U, Zn_U, and ODO).

Despite often being connected with Chl-a in research on water quality management, we found that PhC is not actually correlated with the Chl-a growth in UL, nor is it correlated with P (total or dissolved). PhC is an important consideration in HAB mitigation efforts, as it indicates the presence of potential toxin-producing cyanobacteria. It is well known that cyanobacteria and phytoplankton cell counts are not well correlated, but in UL it would appear that cyanobacteria, like phytoplankton, are also not responding directly to P concentrations, which is contrary to findings on less turbid lakes where nutrient concentrations are a primary driver of both planktonic and cyanobacterial HABs. As cyanobacteria is such a significant management concern, it

would be beneficial to further investigate the complex relationships between phycocyanin and nutrient concentrations, water temperature, and turbidity in UL.

6 Conclusions

Using PCA and MDS analyses and examining distributions in our 61-parameter, 2-year dataset, we advanced the current understanding of UL geochemistry and potential impacts on lake ecology. We also identified areas that could benefit from further research in order to develop more effective HAB management strategies for UL.

We found that total concentrations of Al in UL exceed regulatory criteria when using our analytical methods, although we attribute these elevated levels to nonreactive, clay-dominated suspended sediment. Concentrations of dissolved Al, which would be bioavailable and have the potential to be toxic, were well below regulatory criteria. We consistently measured concentrations of Cu, and P above or very close to regulatory criteria. The high concentrations of P in UL are well known, but the elevated levels of Cu are not widely recognized, and as these metals have the potential to impair the beneficial uses of UL, further studies should be conducted. Cu especially should be considered because of an ongoing program using Cu-based algaecide to treat intense HABs.

Concentrations of other regulated elements remained well below regulatory criteria, which was an interesting result because anthropogenic inputs of these elements to UL have been and may still be large—the low concentrations we observed demonstrate the lake’s high capacity for absorbing and degrading pollutants. Additionally, we found that no regulations for Ba for UL designated uses, but concentrations of Ba are below drinking water limits despite nearby anthropogenic sources.

We found a strong correlation between unfiltered (total) and filtered (dissolved) P, indicating that constant resuspension of P-rich lakebed sediments acts as a source of bioavailable P in the water column. This relationship indicates that dissolved P in the water column is in equilibrium with P sorbed onto sediments and suspended sediments in a sorption dominated system.

PCA groupings indicated that neither phytoplankton, as estimated by Chl-a, nor cyanobacteria, as estimated by PhC, respond directly to bioavailable P. This suggests that water column nutrient concentrations are not the primary driver of algal growth in UL. Other potentially limiting or colimiting micronutrients on UL, including Cu, Ni, and Zn, which had discernable trends that directly opposed the Chl-a trends and correlate with PhC trends.

MDS analysis reinforced the groupings and trends found in the PCA and, in addition, identified three distinct seasonal periods for water column geochemistry in UL: spring (May and June), summer (August), and fall (September). Water column conditions are expected to vary seasonally in response to temperature, light availability, and other influences, so this is not a novel finding—rather, this finding highlights the fact that a comprehensive understanding of UL geochemistry cannot be obtained without monitoring taking place during all seasons and thereby provide information about how UL responds to seasonal changes. This information could help plan the chronological structure of future research.

Our results provide useful information for future studies on UL water quality and help advance the understanding of UL geochemistry necessary to develop and implement efficient and effective HAB management strategies.

References

- [1] G. P. Williams, "Great Salt Lake and Utah Lake Statistical Analysis: Vol II: Utah Lake," 2020, vol. 2.
- [2] E. Snow, "A preliminary study of the algae of Utah Lake: Master's thesis," *Brigham Young University, Provo, Utah, 84p*, 1931.
- [3] W. J. Harding, "The algae of Utah Lake. Part II," *The Great Basin Naturalist*, vol. 31, no. 3, pp. 125-134, 1971.
- [4] S. R. Rushforth and L. E. Squires, "New records and comprehensive list of the algal taxa of Utah Lake, Utah, USA," *The Great Basin Naturalist*, pp. 237-254, 1985.
- [5] L. E. Squires and S. R. Rushforth, "Winter phytoplankton communities of Utah Lake, Utah, USA," *Hydrobiologia*, vol. 131, pp. 235-248, 1986.
- [6] M. C. Whiting, J. D. Brotherson, and S. R. Rushforth, "Environmental interaction in summer algal communities of Utah Lake," *The Great Basin Naturalist*, pp. 31-41, 1978.
- [7] W. J. Harding, "A preliminary report on the algal species presently found in Utah Lake," *The Great Basin Naturalist*, vol. 30, no. 2, pp. 99-105, 1970.
- [8] S. R. Rushforth, L. L. St. Clair, J. A. Grimes, and M. C. Whiting, "Phytoplankton of Utah Lake," *Great Basin Naturalist Memoirs*, pp. 85-100, 1981.
- [9] L. E. Squires, M. C. Whiting, J. D. Brotherson, and S. R. Rushforth, "Competitive displacement as a factor influencing phytoplankton distribution in Utah Lake, Utah," *The Great Basin Naturalist*, pp. 245-252, 1979.
- [10] A. V. Carozzi, "Observations on algal biostromes in the Great Salt Lake, Utah," *The Journal of Geology*, vol. 70, no. 2, pp. 246-252, 1962.
- [11] S. R. Rushforth and G. S. Merkley, "Comprehensive list by habitat of the algae of Utah, USA," *The Great Basin Naturalist*, pp. 154-179, 1988.
- [12] R. Davis, P. Panja, and J. McLennan, "Integrated workflow for interpretation of satellite imageries using machine learning to assess and monitor algal blooms in Utah Lake, USA," *Ecological Informatics*, p. 102033, 2023.
- [13] K. B. Tanner, A. C. Cardall, and G. P. Williams, "A Spatial Long-Term Trend Analysis of Estimated Chlorophyll-a Concentrations in Utah Lake Using Earth Observation Data," *Remote Sensing*, vol. 14, no. 15, p. 3664, 2022.

- [14] C. H. Hansen, S. J. Burian, P. E. Dennison, and G. P. Williams, "Evaluating historical trends and influences of meteorological and seasonal climate conditions on lake chlorophyll a using remote sensing," *Lake and Reservoir Management*, vol. 36, no. 1, pp. 45-63, 2020.
- [15] C. H. Hansen, G. P. Williams, Z. Adjei, A. Barlow, E. J. Nelson, and A. W. Miller, "Reservoir water quality monitoring using remote sensing with seasonal models: case study of five central-Utah reservoirs," *Lake and Reservoir Management*, vol. 31, no. 3, pp. 225-240, 2015.
- [16] S. M. Barrus *et al.*, "Nutrient Atmospheric Deposition on Utah Lake: A Comparison of Sampling and Analytical Methods," *Hydrology*, vol. 8, no. 3, p. 123, 2021.
- [17] J. T. Telfer *et al.*, "Source Attribution of Atmospheric Dust Deposition to Utah Lake," *Hydrology*, vol. 10, no. 11, doi: 10.3390/hydrology10110210.
- [18] M. M. Brown, "Nutrient Loadings to Utah Lake from Bulk Atmospheric Deposition," Masters Masters, Department of Civil and Construction Engineering, Brigham Young University, Provo, Utah, 2023.
- [19] J. G. Reidhead, *Significance of the Rates of Atmospheric Deposition Around Utah Lake and Phosphorus-Fractionation of Local Soils*. Brigham Young University, 2019.
- [20] H. Y. Abu-Hmeidan, G. P. Williams, and A. W. Miller, "Characterizing Total Phosphorus in Current and Geologic Utah Lake Sediments: Implications for Water Quality Management Issues," *Hydrology*, vol. 5, no. 1, p. 8, 2018. [Online]. Available: <https://www.mdpi.com/2306-5338/5/1/8>.
- [21] J. Bradshaw *et al.*, "Chemical response of Utah Lake to nutrient inflow," *Journal (Water Pollution Control Federation)*, pp. 880-887, 1973.
- [22] J. M. Olsen, G. P. Williams, A. W. Miller, and L. Merritt, "Measuring and calculating current atmospheric phosphorous and nitrogen loadings to utah lake using field samples and geostatistical analysis," *Hydrology*, vol. 5, no. 3, p. 45, 2018.
- [23] A. Zanazzi, W. Wang, H. Peterson, and S. H. Emerman, "Using Stable Isotopes to Determine the Water Balance of Utah Lake (Utah, USA)," *Hydrology*, vol. 7, no. 4, p. 88, 2020.
- [24] A. E. Strong, "Remote sensing of algal blooms by aircraft and satellite in Lake Erie and Utah Lake," *Remote sensing of Environment*, vol. 3, no. 2, pp. 99-107, 1974.
- [25] A. Strong, "ERTS-1 observes algal blooms in Lake Erie and Utah Lake," in NASA. *Goddard Space Flight Center Symp. on Significant Results obtained from the ERTS-1, Vol. 1, Sect. A and B*, 1973.
- [26] W. Miller and A. Rango, "Using heat capacity mapping mission (hcmm) data to assess lake water quality 1," *JAWRA Journal of the American Water Resources Association*, vol. 20, no. 4, pp. 493-501, 1984.

- [27] S. R. Schneider, D. F. McGinnis, and J. A. Gatlin, *Use of NOAA/AVHRR visible and near-infrared data for land remote sensing*. US Department of Commerce, National Oceanic and Atmospheric Administration ..., 1981.
- [28] C. H. Hansen and G. P. Williams, "Evaluating remote sensing model specification methods for estimating water quality in optically diverse lakes throughout the growing season," *Hydrology*, vol. 5, no. 4, p. 62, 2018.
- [29] C. H. Hansen, S. J. Burian, P. E. Dennison, and G. P. Williams, "Spatiotemporal variability of lake water quality in the context of remote sensing models," *Remote Sensing*, vol. 9, no. 5, p. 409, 2017.
- [30] S. Rivera, K. Landom, and T. Crowl, "Monitoring macrophytes cover and taxa in Utah Lake by using 2009-2011 Landsat digital imagery," *Revista de Teledetección*, vol. 39, pp. 106-115, 2013.
- [31] Q. Han and Z. Niu, "Construction of the long-term global surface water extent dataset based on water-NDVI spatio-temporal parameter set," *Remote Sensing*, vol. 12, no. 17, p. 2675, 2020.
- [32] B. N. Seegers *et al.*, "Satellites for long-term monitoring of inland US lakes: The MERIS time series and application for chlorophyll-a," *Remote sensing of environment*, vol. 266, p. 112685, 2021.
- [33] W. Zhu, Z. Zhang, Z. Yang, S. Pang, J. Chen, and Q. Cheng, "Spectral probability distribution of closed connected water and remote sensing statistical inference for yellow substance," *Photogrammetric Engineering & Remote Sensing*, vol. 87, no. 11, pp. 807-819, 2021.
- [34] C. H. Hansen, P. Dennison, S. Burian, M. Barber, and G. Williams, "Hindcasting water quality in an optically complex system," *WIT Transactions on Ecology and the Environment*, vol. 209, pp. 35-44, 2016.
- [35] B. P. Page, A. Kumar, and D. R. Mishra, "A novel cross-satellite based assessment of the spatio-temporal development of a cyanobacterial harmful algal bloom," *International journal of applied earth observation and geoinformation*, vol. 66, pp. 69-81, 2018.
- [36] R. D. Ramsey, A. Falconer, and J. R. Jensen, "The relationship between NOAA-AVHRR NDVI and ecoregions in Utah," *Remote Sensing of Environment*, vol. 53, no. 3, pp. 188-198, 1995.
- [37] C. Hansen, N. Swain, K. Munson, Z. Adjei, G. P. Williams, and W. Miller, "Development of sub-seasonal remote sensing chlorophyll-a detection models," *American Journal of Plant Sciences*, vol. 2013, 2013.
- [38] A. C. Cardall, R. C. Hales, K. B. Tanner, G. P. Williams, and K. N. Markert, "LASSO (L1) Regularization for Development of Sparse Remote-Sensing Models with Applications in Optically Complex Waters Using GEE Tools," *Remote Sensing*, vol.

- 15, no. 6, p. 1670, 2023. [Online]. Available: <https://www.mdpi.com/2072-4292/15/6/1670>.
- [39] S. Nofchissey, S. Roberts, J. Hopkinson, J. McDonald, and S. Emerman, "Arsenic and other heavy metals in Utah Lake and its tributaries," 2014.
- [40] X. Zhang, B. Li, H. Xu, M. Wells, B. Tefsen, and B. Qin, "Effect of micronutrients on algae in different regions of Taihu, a large, spatially diverse, hypereutrophic lake," *Water Research*, vol. 151, pp. 500-514, 2019/03/15/ 2019, doi: <https://doi.org/10.1016/j.watres.2018.12.023>.
- [41] R. A. Andersen, *Algal culturing techniques*. Elsevier, 2005.
- [42] T. M. Downs, M. Schallenberg, and C. W. Burns, "Responses of lake phytoplankton to micronutrient enrichment: a study in two New Zealand lakes and an analysis of published data," *Aquatic Sciences*, vol. 70, pp. 347-360, 2008.
- [43] L. Norman, D. J. E. Cabanes, S. Blanco-Ameijeiras, S. A. M. Moisset, and C. S. Hassler, "Iron Biogeochemistry in Aquatic Systems: From Source to Bioavailability," *CHIMIA*, vol. 68, no. 11, p. 764, 11/26 2014, doi: 10.2533/chimia.2014.764.
- [44] M. Krivokapić, "Study on the Evaluation of (Heavy) Metals in Water and Sediment of Skadar Lake (Montenegro), with BCF Assessment and Translocation Ability (TA) by *Trapa natans* and a Review of SDGs," *Water*, vol. 13, no. 6, p. 876, 2021. [Online]. Available: <https://www.mdpi.com/2073-4441/13/6/876>.
- [45] J. G. Rueter and R. R. Petersen, "Micronutrient effects on cyanobacterial growth and physiology," *New Zealand Journal of Marine and Freshwater Research*, vol. 21, no. 3, pp. 435-445, 1987/09/01 1987, doi: 10.1080/00288330.1987.9516239.
- [46] T. K. Bayer, M. Schallenberg, and C. E. Martin, "Investigation of nutrient limitation status and nutrient pathways in Lake Hayes, Otago, New Zealand: a case study for integrated lake assessment," *New Zealand Journal of Marine and Freshwater Research*, vol. 42, no. 3, pp. 285-295, 2008.
- [47] M. Dengg *et al.*, "Growth at the limits: comparing trace metal limitation of a freshwater cyanobacterium (*Dolichospermum lemmermannii*) and a freshwater diatom (*Fragilaria crotonensis*)," *Scientific Reports*, vol. 12, no. 1, p. 467, 2022/01/10 2022, doi: 10.1038/s41598-021-04533-9.
- [48] J. A. Facey, T. A. Rogers, S. C. Apte, and S. M. Mitrovic, "Micronutrients as growth limiting factors in cyanobacterial blooms; a survey of freshwaters in South East Australia," *Aquatic Sciences*, vol. 83, no. 2, p. 28, 2021/02/19 2021, doi: 10.1007/s00027-021-00783-x.
- [49] J. A. Facey, S. C. Apte, and S. M. Mitrovic, "A Review of the Effect of Trace Metals on Freshwater Cyanobacterial Growth and Toxin Production," *Toxins*, vol. 11, no. 11, p. 643, 2019. [Online]. Available: <https://www.mdpi.com/2072-6651/11/11/643>.

- [50] Patricia Shaw-Allen and G.W.Sutler. "Metals." US EPA. <https://www.epa.gov/caddis-vol2/metals> (accessed 2/27, 2023).
- [51] M. S. Schuler and R. A. Relyea, "A Review of the Combined Threats of Road Salts and Heavy Metals to Freshwater Systems," *BioScience*, vol. 68, no. 5, pp. 327-335, 2018, doi: 10.1093/biosci/biy018.
- [52] C. Monchanin, J.-M. Devaud, A. B. Barron, and M. Lihoreau, "Current permissible levels of metal pollutants harm terrestrial invertebrates," *Science of The Total Environment*, vol. 779, p. 146398, 2021/07/20/ 2021, doi: <https://doi.org/10.1016/j.scitotenv.2021.146398>.
- [53] C. L. Mogren and J. T. Trumble, "The impacts of metals and metalloids on insect behavior," *Entomologia Experimentalis et Applicata*, vol. 135, no. 1, pp. 1-17, 2010.
- [54] P. S. Rainbow, "Trace metal concentrations in aquatic invertebrates: why and so what?," *Environmental Pollution*, vol. 120, no. 3, pp. 497-507, 2002/12/01/ 2002, doi: [https://doi.org/10.1016/S0269-7491\(02\)00238-5](https://doi.org/10.1016/S0269-7491(02)00238-5).
- [55] H. Marschner, *Marschner's mineral nutrition of higher plants*. Academic press, 2011.
- [56] J. E. Gall, R. S. Boyd, and N. Rajakaruna, "Transfer of heavy metals through terrestrial food webs: a review," *Environmental Monitoring and Assessment*, vol. 187, no. 4, p. 201, 2015/03/24 2015, doi: 10.1007/s10661-015-4436-3.
- [57] A. S. Ali and A. R. US SA, "Effect of different heavy metal pollution on fish," *Res. J. Chem. Environ. Sci*, vol. 2, no. 1, pp. 74-79, 2014.
- [58] P. A. Amundsen, F. J. Stalvik, A. A. Lukin, N. A. Kashulin, O. A. Popova, and Y. S. Reshetnikov, "Heavy metal contamination in freshwater fish from the border region between Norway and Russia," (in eng), *Sci Total Environ*, vol. 201, no. 3, pp. 211-24, Aug 18 1997, doi: 10.1016/s0048-9697(97)84058-2.
- [59] M. Lucia, J.-M. André, K. Gontier, N. Diot, J. Veiga, and S. Davail, "Trace element concentrations (mercury, cadmium, copper, zinc, lead, aluminium, nickel, arsenic, and selenium) in some aquatic birds of the Southwest Atlantic Coast of France," *Archives of Environmental Contamination and Toxicology*, vol. 58, no. 3, pp. 844-853, 2010.
- [60] J. Burger and M. Gochfeld, "Behavioral impairments of lead-injected young herring gulls in nature," *Toxicological sciences*, vol. 23, no. 4, pp. 553-561, 1994.
- [61] A. Scheuhammer, "The chronic toxicity of aluminium, cadmium, mercury, and lead in birds: a review," *Environmental Pollution*, vol. 46, no. 4, pp. 263-295, 1987.
- [62] E. Epstein and A. J. Bloom, *Mineral nutrition of plants: principles and perspectives*. Sinauer, 1853.
- [63] J. S. Cavet, G. P. Borrelly, and N. J. Robinson, "Zn, Cu and Co in cyanobacteria: selective control of metal availability," *FEMS Microbiology Reviews*, vol. 27, no. 2-3, pp. 165-181, 2003.

- [64] P. Chakraborty, P. R. Babu, T. Acharyya, and D. Bandyopadhyay, "Stress and toxicity of biologically important transition metals (Co, Ni, Cu and Zn) on phytoplankton in a tropical freshwater system: An investigation with pigment analysis by HPLC," *Chemosphere*, vol. 80, no. 5, pp. 548-553, 2010.
- [65] C. Moreno-Vivián, P. n. Cabello, M. Martínez-Luque, R. Blasco, and F. Castillo, "Prokaryotic nitrate reduction: molecular properties and functional distinction among bacterial nitrate reductases," *Journal of bacteriology*, vol. 181, no. 21, pp. 6573-6584, 1999.
- [66] R. Axler, R. Gersberg, and C. Goldman, "Stimulation of nitrate uptake and photosynthesis by molybdenum in Castle Lake, California," *Canadian journal of fisheries and aquatic sciences*, vol. 37, no. 4, pp. 707-712, 1980.
- [67] H. Ali, E. Khan, and I. Ilahi, "Environmental Chemistry and Ecotoxicology of Hazardous Heavy Metals: Environmental Persistence, Toxicity, and Bioaccumulation," *Journal of Chemistry*, vol. 2019, p. 6730305, 2019/03/05 2019, doi: 10.1155/2019/6730305.
- [68] L. Merritt and W. Miller, "Nutrient loading to Utah Lake," *Utah Lake Studies*, 2016.
- [69] U. S. C. Bureau. "US Census Bureau Publications - Census of Population and Housing." <https://www.census.gov/prod/www/decennial.html> (accessed October, 2021, 2021).
- [70] C. L. Whetten, "'This strange enterprise': Geneva steel and the American west," M.A., The University of Utah, United States -- Utah, 1502698, 2011. [Online]. Available:http://www.lib.byu.edu/jfinder.pl??url_ver=Z39.88-2004&rft_val_fmt=info:ofi/fmt:kev:mtx:dissertation&genre=dissertations&sid=ProQ:ProQuest+Dissertations+26+Theses+Global&atitle=&title=%E2%80%9CThis+strange+enterprise%E2%80%9D%3A+Geneva+steel+and+the+American+west&issn=&date=2011-01-01&volume=&issue=&spage=&au=Whetten%2C+Craig+Loal&isbn=978-1-267-05922-2&jtitle=&btitle=&rft_id=info:eric/&rft_id=info:doi/
- [71] R. Williams *et al.*, "Human-Driven Trophic Changes in a Large, Shallow Urban Lake: Changes in Utah Lake, Utah from Pre-European Settlement to the Present," *Water, Air, & Soil Pollution*, vol. 234, no. 4, p. 218, 2023/03/22 2023, doi: 10.1007/s11270-023-06228-5.
- [72] D. K. Fuhriman, L. B. Merritt, A. W. Miller, and H. S. Stock, "Hydrology and Water Quality of Utah Lake," *Great Basin Naturalist Memoirs*, no. 5, pp. 43-67, 1981. [Online]. Available: <http://www.jstor.org/stable/23376546>.
- [73] L. Schoderboeck, S. Mühlegger, A. Losert, C. Gausterer, and R. Hornek, "Effects assessment: Boron compounds in the aquatic environment," *Chemosphere*, vol. 82, no. 3, pp. 483-487, 2011/01/01/ 2011, doi: <https://doi.org/10.1016/j.chemosphere.2010.10.031>.

- [74] A. Norici, R. Hell, and M. Giordano, "Sulfur and primary production in aquatic environments: an ecological perspective," *Photosynthesis Research*, vol. 86, no. 3, pp. 409-417, 2005/12/01 2005, doi: 10.1007/s11120-005-3250-0.
- [75] J. Karjalainen *et al.*, "Sulfate sensitivity of aquatic organism in soft freshwaters explored by toxicity tests and species sensitivity distribution," *Ecotoxicology and Environmental Safety*, vol. 258, p. 114984, 2023/06/15/ 2023, doi: <https://doi.org/10.1016/j.ecoenv.2023.114984>.
- [76] M. Bodzek, "The removal of boron from the aquatic environment-state of the art," *Desalination and Water Treatment*, vol. 57, no. 3, pp. 1107-1131, 2016/01/14 2016, doi: 10.1080/19443994.2014.1002281.
- [77] S. C. Gad, "Barium," in *Encyclopedia of Toxicology (Third Edition)*, P. Wexler Ed. Oxford: Academic Press, 2014, pp. 368-370.
- [78] K. N. Constenius, D. L. Clark, J. K. King, and J. B. Ehler, ed. Salt Lake City, UT, USA: Utah Geological Survey,, 2011.
- [79] L. F. Hintze and B. J. Kowallis, *Geologic History of Utah: A Field Guide to Utah's Rocks*, Special Publications 9 ed. Provo, UT, USA: Department of Geological Sciences, Brigham Young University, 2009.
- [80] S. Szklarek, A. Górecka, and A. Wojtal-Frankiewicz, "The effects of road salt on freshwater ecosystems and solutions for mitigating chloride pollution - A review," *Science of The Total Environment*, vol. 805, p. 150289, 2022/01/20/ 2022, doi: <https://doi.org/10.1016/j.scitotenv.2021.150289>.
- [81] K. J. Maier and A. W. Knight, "Ecotoxicology of selenium in freshwater systems," (in eng), no. 0179-5953 (Print).
- [82] X. Diaz, W. P. Johnson, and D. L. Naftz, "Selenium mass balance in the Great Salt Lake, Utah," *Science of the Total Environment*, vol. 407, no. 7, pp. 2333-2341, 2008.
- [83] Utah Department of Environmental Quality. "Standards of Quality for Waters of the State." <https://documents.deq.utah.gov/water-quality/standards-technical-services/DWQ-2021-017555.pdf> (accessed.
- [84] Utah Department of Environmental Quality Division of Water Quality. "Water Quality Standards - Utah Department of Environmental Quality." <https://deq.utah.gov/water-quality/water-quality-standards> (accessed.
- [85] U. D. o. E. Quality. "Water Qulaity Assessment and Analysis: Utah Lake Water Quality Study " Utah Department of Water Quality <https://deq.utah.gov/water-quality/water-quality-assessment-and-analysis-utah-lake> (accessed 2024).
- [86] J. V. Laan, "Question about interpreting R317-2 water quality standards ", K. Tanner, Ed., ed, 2022.
- [87] R. Valek, E. Walmer, C. Dorrett, K. Tanner, A. Cardall, and G. Williams, "Utah Lake Nutrient Cycling Studies: Limnnocorral Usage and Experiments," presented

- at the Intermountain Engineering, Technology, and Computing (IETC), Orem, UT, USA, 2022. [Online]. Available: <https://ieeexplore.ieee.org/document/9796864>.
- [88] C. Dorrett, A. Cardall, K. Tanner, R. Valek, and G. Williams, "Data Collection Methods for Utah Lake Nutrient Cycling Study," American Water Works Association Intermountain Section Poster, October 2021, 2021.
- [89] YSI. *ProDIGITAL User Manual*.
- [90] B. O. R. United States. "Historic Data." Bureau of Reclamation. <https://www.usbr.gov/rsrvWater/HistoricalApp.html> (accessed 1/15, 2024).
- [91] YSI. "ProDSS ODO Optical Dissolved Oxygen Sensor." <https://www.ysi.com/product/id-626900/prodss-odo-optical-dissolved-oxygen-sensor> (accessed 2024).
- [92] YSI. "ProDSS Turbidity Sensor." https://www.ysi.com/product/id-626901/prodss-turbidity-sensor?gad_source=1&gclid=CjwKCAjw17qvBhBrEiwA1rU9w9A1JgfW_K8z2xRdulWvMRh4EgTzViCGRdOwKj6KyBtkcVNRZfN8xoCCB0QAvD_BwE (accessed 2024).
- [93] YSI. "ProDSS Conductivity and Temperator Sensor." <https://www.ysi.com/product/id-626902/prodss-conductivity-and-temperature-sensor> (accessed 2024).
- [94] YSI. "ProDSS pH/ORP Sensor with Module" <https://www.ysi.com/product/id-626904/prodss-phorp-sensor-with-module> (accessed 2024).
- [95] YSI. "ProDSS Total Algae PC Sensor." <https://www.ysi.com/pro/talpc> (accessed 2024).
- [96] A. J. Horowitz, K. A. Elrick, and M. R. Colberg, "The effect of membrane filtration artifacts on dissolved trace element concentrations," *Water Research*, vol. 26, no. 6, pp. 753-763, 1992/06/01/ 1992, doi: [https://doi.org/10.1016/0043-1354\(92\)90006-P](https://doi.org/10.1016/0043-1354(92)90006-P).
- [97] M. C. Randall, "Characterizing the Fate and Mobility of Phosphorus in Utah Lake Sediments," MS, Physical and Mathematical Sciences; Geological Sciences, Brigham Young University, 2017. [Online]. Available: <https://scholarsarchive.byu.edu/etd/6915/>
- [98] EPA, "2018 Final Aquatic Life Criteria for Aluminum in Freshwater," (in English), US EPA, 2022. [Online]. Available: <https://www.epa.gov/wqc/2018-final-aquatic-life-criteria-aluminum-freshwater>.
- [99] D. L. Correll, "The role of phosphorus in the eutrophication of receiving waters: A review," *Journal of environmental quality*, vol. 27, no. 2, pp. 261-266, 1998.
- [100] PSOMAS, "Utah Lake TMDL: Pollutant Loading Assessment & Designated Beneficial Use Impairment Assessment," Department of Environmental Quality 2007. [Online]. Available: <https://documents.deq.utah.gov/legacy/programs/water->

quality/watersheds/docs/2009/02Feb/Final_Draft_Task2_Task3_Memo%20_08-01-07.pdf

- [101] W. H. Brimhall and L. B. Merritt, "Geology of Utah Lake: Implications for resource management," *Great Basin Naturalist Memoirs*, pp. 24-42, 1981.
- [102] JMP Statistical Discovery LLC. "Principal Component Report Options." <https://www.jmp.com/support/help/en/17.2/index.shtml#page/jmp/principal-components-report-options.shtml> (accessed 2024).
- [103] A. Geron, *Hands-On Machine Learning with Scikit-Learn, Keras, and TensorFlow: Concepts, Tools, and Techniques to Build Intelligent Systems*. O'Reilly Media, Inc., 2019.
- [104] A. H. Welch, D. Westjohn, D. R. Helsel, and R. B. Wanty, "Arsenic in ground water of the United States: occurrence and geochemistry," *Groundwater*, vol. 38, no. 4, pp. 589-604, 2000.
- [105] N. E. Korte M.S and Q. Fernando Ph.D, "A review of arsenic (III) in groundwater," *Critical Reviews in Environmental Control*, vol. 21, no. 1, pp. 1-39, 1991/01/01 1991, doi: 10.1080/10643389109388408.
- [106] W. McKinney, "Data structures for statistical computing in python," in *Proceedings of the 9th Python in Science Conference*, 2010, vol. 445, no. 1: Austin, TX, USA, pp. 51-56.
- [107] W. S. Torgerson, "Multidimensional scaling: I. Theory and method," *Psychometrika*, vol. 17, no. 4, pp. 401-419, 1952/12/01 1952, doi: 10.1007/BF02288916.
- [108] M. A. A. Cox and T. F. Cox, "Multidimensional Scaling," in *Handbook of Data Visualization*. Berlin, Heidelberg: Springer Berlin Heidelberg, 2008, pp. 315-347.
- [109] E. K. Jackson, W. Roberts, B. Nelsen, G. P. Williams, E. J. Nelson, and D. P. Ames, "Introductory overview: Error metrics for hydrologic modelling – A review of common practices and an open source library to facilitate use and adoption," *Environmental Modelling & Software*, vol. 119, pp. 32-48, 2019/09/01/ 2019, doi: <https://doi.org/10.1016/j.envsoft.2019.05.001>.
- [110] JMP Statistical Discovery LLC. "Fit Details." <https://www.jmp.com/support/help/en/17.2/index.shtml#page/jmp/fit-details-2.shtml#ww344966> (accessed March 4th 2024).
- [111] (2021). *Utah Lake Marina HAB Treatments Evaluation of Treatment Effectiveness 2021 Interim Report* [Online] Available: <https://documents.deq.utah.gov/water-quality/standards-technical-services/harmful-algal-blooms/DWQ-2022-002008.pdf>
- [112] (2023). *Utah Lake Authority FY 2023 Annual Monitoring Report* [Online] Available: <https://le.utah.gov/interim/2023/pdf/00004529.pdf>
- [113] M. C. Randall *et al.*, "Sediment potentially controls in-lake phosphorus cycling and harmful cyanobacteria in shallow, eutrophic Utah Lake," *PLoS One*, vol. 14, no. 2, p. e0212238, 2019.

- [114] J. B. Taggart *et al.*, "Historical Phosphorus Mass and Concentrations in Utah Lake: A Case Study with Implications for Nutrient Load Management in a Sorption-Dominated Shallow Lake," *Water*, vol. 16, no. 7, p. 933, 2024. [Online]. Available: <https://www.mdpi.com/2073-4441/16/7/933>.
- [115] US EPA, "Consumer Factsheet on: Barium ". [Online]. Available: <https://archive.epa.gov/water/archive/web/pdf/archived-consumer-fact-sheet-on-barium.pdf>
- [116] US EPA. "National Primary Drinking Water Regulations " <https://www.epa.gov/ground-water-and-drinking-water/national-primary-drinking-water-regulations> (accessed 2024).

Appendix

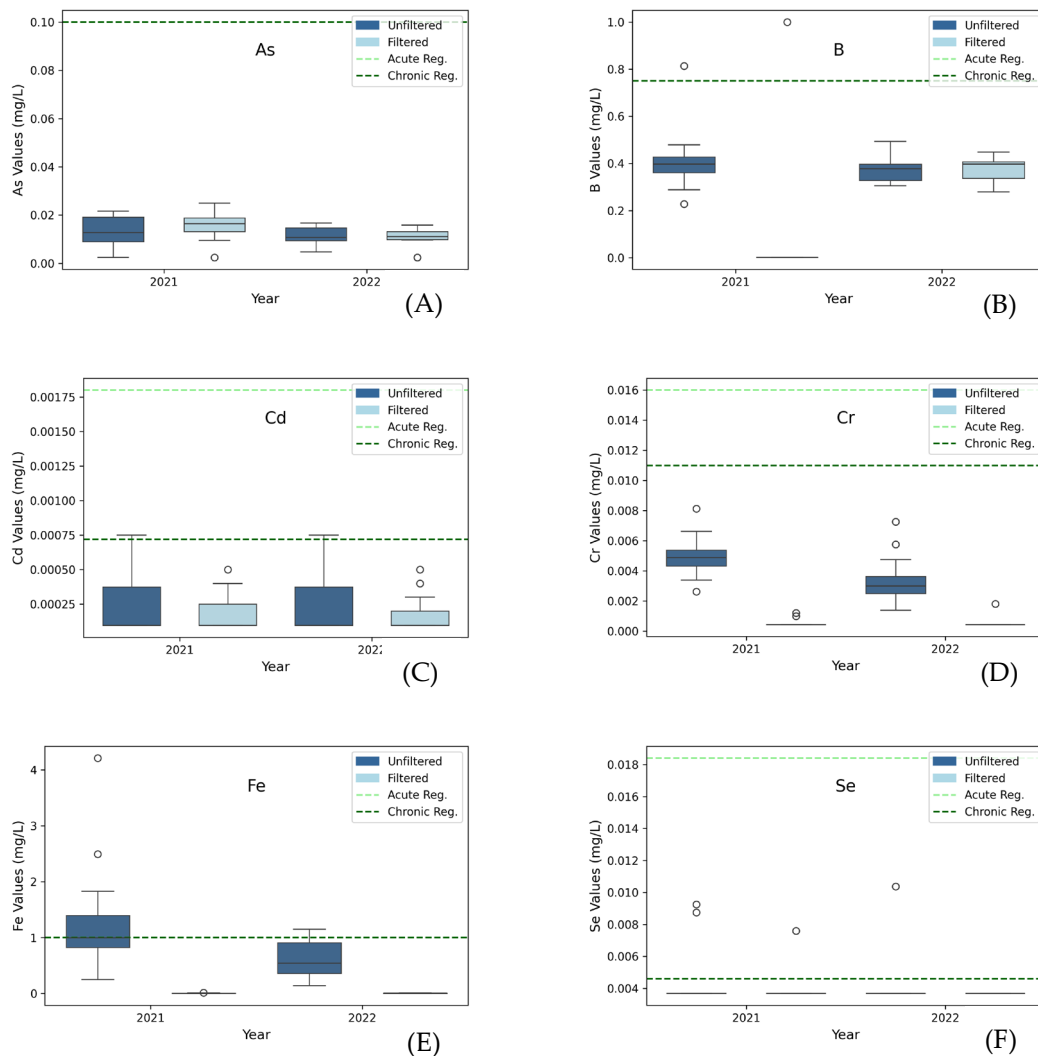


Figure A-1. Distributions of (A) As, (B) B, (C) Cd, (D) Cr, (E) Fe, and (F) Se grouped by year, 2021 and 2022; and phase, unfiltered (dark blue) and filtered (light blue) with reference lines for acute and chronic regulatory levels.